The impacts of longitudinal separation, efficiency loss and cruise speed adjustment in robust terminal traffic flow problem under uncertainty

Kam K.H. NG [a], Felix T.S. CHAN [b,*], Yichen QIN [c], Gangyan Xu [a]

[a] *Department of Aeronautical and Aviation Engineering, The Hong Kong Polytechnic University, Hung Hom, Hong Kong SAR, China*

[b] *Department of Decision Sciences, Macau University of Science and Technology, Avenida Wai Long, Taipa, Macau.*

[c] *School of Economics and Management, Shanghai Maritime University, Shanghai, 201306, China*

* *Corresponding author.*

Email Address: kam.kh.ng@polyu.edu.hk (Kam K.H. NG), tschan@must.edu.mo (Felix T.S. CHAN), ycqin@shmtu.edu.cn (Yichen QIN), gangyan.xu@polyu.edu.hk (Gangyan Xu)

Acknowledgment

The research is supported by the Research Grants Council, the Hong Kong Government (Grant number PolyU25218321), The Natural Science Foundation of China (Grant number 72101144, 71971143); the Research Committee of The Hong Kong Polytechnic University (Project number BE3V, G-YBFD and G-YBN1) and Shanghai Pujiang Programme (2021PJC067).

Declarations of interest: The authors declare that they have no known competing financial interests or personal relationships that could have appeared to influence the work reported in this paper.

The impacts of longitudinal separation, efficiency loss and cruise speed adjustment in robust terminal traffic flow problem under uncertainty

Abstract

Minimisation of approaching time and maximisation of the utilisation of air route and airport resources are the two ultimate goals of air traffic control. This research considers the problem of decision-making in the terminal manoeuvring area during the uncertain arrival times at entry waypoints of flights and investigates the air traffic controller specific parameters in the model. The two-stage optimisation framework will first determine a deterministic schedule and optimise the approaching time and arrival time on runways while considering additional longitudinal separation, efficiency loss from deterministic schedule and cruise speed adjustment in the second-stage optimisation model via sample average approximation (SAA). The numerical experiments were performed with the support of real-world data, and the results suggested an efficiency loss of 20%, which can absorb the empirical probabilistic lateness at entry waypoints. The proposed method could determine the estimated average delay time at runways with different settings of additional buffer for longitudinal separation requirement and trade-off parameters between the estimated average delay time at runways and estimated penalty cost of cruise speed adjustment.

Keywords: robust schedule design; air traffic control; sample average approximation; optimisation; aviation.

1. Introduction

1.1. Problem description

In this paper, we examine a robust schedule design for terminal traffic flow problem (TTFP), which is defined as the problem of designing a conflict resolution and coordinating various air traffic resources, including air route, aeronautical holding, arrival segments, joint segments, common guided path and runways, with the aim of developing an optimal air route network with efficient air traffic movement in the terminal manoeuvring area (TMA). An increase in air traffic load raises the possibility of air route congestion in the TMA. Thus, re-scheduling of flights is required in various situations by Air Traffic Control (ATC), such as during air traffic delay and adverse weather conditions (Wee, Lye, & Pinheiro, 2018). Additionally, aeronautical holding and approach path decisions are usually subjected to the current air traffic situation and traffic control regulations, which leads to complicated and dynamic air traffic flow management (C. K. M. Lee et al., 2018; K. K. H. Ng, Lee, Chan, & Qin, 2017).

The volume of air transportation has been increasing significantly in recent years due to the increasing number of passengers and airlines (K. K. H. Ng, Lee, Chan, & Lv, 2018; Qin, Chan, Chung, Qu, & Niu, 2018). Air traffic networks are becoming increasingly complicated as well (Farhadi, Ghoniem, & Al-Salem, 2014; Gelhausen, Berster, & Wilken, 2013). As a result, most international airports have experienced heavy air traffic delays in the past two decades. An increase in expenses for crews, fuel, maintenance and gross profit may be the consequences of flight delays (M. Ball et al., 2010; Lu, Zhu, Han, & Hu, 2019; Qin, Wang, Chan, Chung, & Qu, 2018, 2019). Hence, airport capacity management is of utmost importance to deal with issues in terms of ATC resource allocation (M. O. Ball, Hansen, Swaroop, & Zou, 2013; Nikoleris & Hansen, 2012). In practical situations, since the actual flight arrival/departure time may deviate from the predetermined or estimated time due to exogenous uncertainty (K. K. H. Ng et al., 2017), it is essential to design an appropriate model for ATC by fulfilling its current needs. This is emphasised by Artiouchine, Baptiste, and Dürr (2008) and Eun, Hwang, and Bang (2010), who considered discrete holding patterns and airborne delays in their models to design smooth landing schedules. Peterson, Neels, Barczi, and Graham (2013) indicate that the major cause for delays is usually the lack of TMA capacity. Additionally, air traffic congestion and flight delays occur frequently at busy airports, which might be attributed to the low efficiency of ATC (Samà, D'Ariano, D'Ariano, & Pacciarelli, 2017). (Samà, D'Ariano, D'Ariano, et al., 2017). Terminal traffic flow capacity deficiencies might cause delayed propagation in the subsequent TMA activities (Kafle & Zou, 2016; Pyrgiotis, Malone, & Odoni, 2013). Therefore, airport capacity management is crucial to deal with issues in terms of ATC resource allocation (Nikoleris & Hansen, 2012). It is also important for ATC to provide detailed commands to pilots regarding the approaching and aeronautical holding decisions (Samà, D'Ariano, Corman, & Pacciarelli, 2017; Samà, D'Ariano, D'Ariano, et al., 2017; L. Xu, Zhang, Xiao, & Wang, 2017). Moreover, the total approaching time of a flight in TMA, TMA throughput might be affected by metrological conditions and route traffic situations (X. Chen et al., 2020; Pohl, Kolisch, & Schiffer, 2020; Yang, Gao, & He, 2020). In practice, since the actual flight arrival/departure time might deviate from the predetermined or estimated time due to exogenous uncertainty, it is essential to design an appropriate model for ATC by fulfilling its current needs. The uncertain variables are designed based on a probability-known distribution using historical data (X. Chen et al., 2020; Jacquillat, Odoni, & Webster, 2017).

In order to enhance the level of practical usage and the robustness of the solution, a detailed control of the ATC practices, including air segments, holding patterns and landing operations, is required to provide aid and assistance in resolving potential conflicts and offering collision-free guidance to all flights within a TMA (Givoni & Chen, 2017; Qian, Mao, Chen,

Chen, & Yang, 2017). Any accident due to improper terminal resource usage would cause dramatic loss, disrupt airport operations, have adverse effects on subsequent activities and delay propagation (Sinclair, Cordeau, & Laporte, 2014). Therefore, the TTFP schedule should inherently include a certain degree of robustness. A robust scheduling approach for airport operations should perform appropriately even when the time required for operations is uncertain, which increases the vulnerability of disruption of airside operations. In fact, the management of flight approaching and departing procedures are key components of an efficient air transportation system (Gillen, Jacquillat, & Odoni, 2016).

1.2. Literature review

The TTFP is an extension of the Aircraft Sequencing and Scheduling Problem (ASSP) (K. K. H. Ng et al., 2018). The ASSP model offers a microscopic view of the traffic flow framework. It mainly considers runway assignments and sequencing problems that are constrained by the capacity of the available runway resources, safety and the efficient allocation of landing directions and positions in a multi-runway system (Deng et al., 2018; K. K. H. Ng et al., 2017). However, the final approach operations are also affected by the manner of the ATCOs at the TMA (Hansen & Zou, 2013; Zou & Hansen, 2012). For example, inefficient terminal ATC and poor management of the approach route selection may lead to TMA capacity being uncaptured (C. K. Lee, Zhang, & Ng, 2019; Samà, D'Ariano, D'Ariano, et al., 2017). Nonetheless, increasing the number of aeronautical holdings further increases the possibility of flight delays, ASSP re-scheduling and extra fuel consumption (Artiouchine et al., 2008). ATC and airspace congestion control are the most interesting research directions warranting attention. As the airport network, approach fix and terminal traffic route are predetermined, the relevant studies can be classified into different classes of mathematical modelling, including discrete-time network approach (Balakrishnan & Chandran, 2010), time-space network approach (Bertsimas, Lulli, & Odoni, 2011; Kafle & Zou, 2016; Yang et al., 2020), graph theory (Samà, D'Ariano, Corman, et al., 2017; Samà, D'Ariano, D'Ariano, et al., 2017) and rolling horizon method (Prakash, Piplani, & Desai, 2018; Samà, D'Ariano, & Pacciarelli, 2013b). Extensive research has been conducted in the past decade to address the terminal traffic flow and airspace congestion control, including the resolutions and decisions on runway configuration (Gillen et al., 2016; Jacquillat & Odoni, 2015a, 2015b, 2018; Jacquillat et al., 2017), runway scheduling (Heidt, Helmke, Kapolke, Liers, & Martin, 2016; Lieder, Briskorn, & Stolletz, 2015; Lieder & Stolletz, 2016; Prakash et al., 2018), approach route (Samà, D'Ariano, Corman, & Pacciarelli, 2018; Samà, D'Ariano, D'Ariano, et al., 2017; Toratani, 2019), waypoint merge system (Youkyung Hong, Choi, & Kim, 2018; Y. Hong, Choi, Lee, & Kim, 2018), aeronautical holding (Samà, D'Ariano, Corman, et al., 2017), fuel consumption (Khan, Chung, Ma, Liu, & Chan, 2019), runway and waypoint arrival time determination (Liang, Delahaye, & Marechal, 2018; Murça, Hansman, Li, & Ren, 2018). In order to provide complementary information on ATC at a TMA, Bianco, Dell'Olmo, and Giordani (1997) proposed the formulation of TTFP, which uses a no-wait job-shop scheduling method. Artiouchine et al. (2008) and Eun et al. (2010) also considered the absorption of airborne delays by determining the number of aeronautical holdings for approaching flights. Moreover, Samà, D'Ariano, D'Ariano, and Pacciarelli (2014) proposed a novel alternative graph approach to the TTFP. Alternatively a rolling horizon method for TTFP problem proved to be able to trim the problem into several subproblems (Samà, D'Ariano, & Pacciarelli, 2013a). The structure of the TTFP is also subjected to the actual air traffic network, air segment structure, wind direction and the terrain constraints near a TMA. The deterministic nature of the TTFP model has been well studied in relation to a conflict-free approach and the minimisation of total flow time within a TMA. However, computational loading using a no-wait job-shop scheduling, rolling horizon or alternative graph approach has proven to be significant in practical use.

Various approaches in managing ATC decisions under the dynamic changes of the environment were proposed in the literature of the ASSP model. It is noteworthy that solving such large-scale TTFP and airport arrival demand management are computationally intractable and fail to meet the industrial needs in near-time decisions. The model might involve complex constraints with regard to the air route and airport geographical structure, runway orientation and slope, aeronautical holding stack level and meteorological conditions. The contemporary research in traffic flow management focuses on the recovery approach, which is a reactive approach that handles delays when they arise (Z. Liang et al., 2018). Stochastic and robust scheduling are proactive approaches that avoid delay propagation and fault-driven re-scheduling efforts when delays occur over a particular period (Gehlot, Honnappa, & Ukkusuri, 2020; Tang & Wang, 2020; Yan & Chen, 2021). Additionally, the uncertainty in air traffic flow management increases the complexity of ATC modelling (K. K. H. Ng et al., 2017). In terms of the stochastic approach, the uncertain variables are designed based on a probability-known distribution using historical data (Jacquillat & Odoni, 2015a, 2015b; Jacquillat, Odoni, & Webster, 2016). However, the expected outcome may not be derived from historical records in certain situations. In contrast, robust modelling is a risk-averse approach that deals with conservative decision-making (K. K. H. Ng et al., 2017). Robust optimisation in an optimisation approach that handles the ambiguous distribution of uncertainty and is used to estimate the possible outcome without precise measurements on uncertain parameters (Habibi, Battaïa, Cung, Dolgui, & Tiwari, 2019; He, Guan, Xu, Yue, & Ullah, 2020; Hu, Ng, & Qin, 2016; Maiyar & Thakkar, 2019). The robust approach considers a possible deviation as an interval-based uncertainty while developing the robust performance instead of considering the statistical control of uncertainty distribution (K. K. H. Ng, C. K. M. Lee, F. T. S. Chan, C.-H. Chen, & Y. Qin, 2020b; K. K. H. Ng et al., 2017). Therefore, a robust schedule design approach is desirable in a complex environment (Qiu, Sun, & Sun, 2020).

The ambiguity aversion, in economics literature, is referred to as that the decision maker and tends to prefer known risk over unknown risk or uncertainty (Epstein, 1999; Gilboa & Schmeidler, 1989; Schmeidler, 1989). Ben-Tal, Bertsimas, and Brown (2010) first developed the soft robust model for convex optimisation under ambiguity aversion. The conservativeness of solutions under the convex risk measure guarantees that the solution quality is against the downside performance in terms of uncertainty in convex optimisation (Bertsimas, Nohadani, & Teo, 2010). Furthermore, the estimation of unknown parameters in robust optimisation usually falls into interval cases. In this regard, the robust solution is deemed to be too conservative but less vulnerable to disruption (De La Vega, Munari, & Morabito, 2020). It is not possible to monitor closely when dealing with delay estimations for all approaching flights. The choice of robust optimisation methods is subject to the preference and the balance between the levels of disruption and resilience (Aissi, Bazgan, & Vanderpooten, 2009). Absolute robustness, robust deviation and relative deviation are well-known robust optimisation methods (X. Xu, Cui, Lin, & Qian, 2013). The aim of robust optimisation is to neutralise the outcome of uncertainty if wrong decisions create a dramatic failure in operations (Basso, 2008; Delavernhe, Lersteau, Rossi, & Sevaux, 2020). K. K. H. Ng et al. (2017) proposed a min-max regret approach with regard to hedging the arrival and departure uncertainty under the worst-case scenario in order to develop a robust ASSP schedule for a mix-mode parallel runway operation.

An efficient terminal traffic flow solution can improve both the airlines' and airports' performances (García-Heredia, Alonso-Ayuso, & Molina, 2019; Samà, D'Ariano, D'Ariano, et al., 2017). Even for flights that enter a TMA, the total approaching time may be affected by weather conditions and route traffic situations. Furthermore, inaccurate information regarding the approaching time and approaching route may leads to infeasibility of the planned schedule and, sometimes, leads to re-scheduling efforts by the ATC (K. K. H. Ng et al., 2017; Zheng et al., 2019). Moreover, terminal traffic flow capacity deficiencies may cause delay propagation in the subsequent runway activities (Campanelli et al., 2016; Churchill, Lovell, & Ball, 2010; Kafle & Zou, 2016; Pyrgiotis et al., 2013). Therefore, the effect of aggregate delays should not be underestimated. Instead of developing a reassignment method and recovery approach (Vink, Santos, Verhagen, Medeiros, & Filho, 2020) to partially absorb the effect of the disrupted schedule, a robust schedule design for TTFP can optimise a pre-tactical schedule for TTFP (30-minutes to 1-hour scheduling decision in advanced before the actual operations). The pre-tactical schedule decision can help ATCOs to determine a solution that is vulnerable to disruption. Air traffic synchronisation and continuous descent operations (CDO) can maximise the air traffic movement and regain efficiency by modelling the flight trajectory and descending profile (Sáez et al., 2021; Sáez, Prats, Polishchuk, & Polishchuk, 2020). The study on vertical and flight speed profile can further support the arrival manager (AMAN) model to achieve better separation standard and air traffic movement with respect to various meteorological conditions. Although the uncertain events only existed when the impact of uncertain parameters is revealed, we can expect that the robust schedule for TTFP is well protected against the uncertain arrival time on entry waypoints. In this regard, when in actual operations, the robust solution for TTFP is much more stability and low possibility of being interrupted and required re-scheduling effort in real time. The computations on worst case analysis in robust optimisation can be time consuming, which leads to a lower level of practical usage in real-world scenarios. Therefore, a robust schedule design for TTFP is proposed to mitigate the effect of delay propagation by introducing uncertain variable(s) in the robust TTFP schedule (Marla, Vaze, & Barnhart, 2018) and offers a quick solution for feasible cruise speed planning in hedging air traffic delays via scenario analysis.

1.3. Contribution of the research

Insufficient research is available on simplified and analytical mathematical models to formulate sophisticated interactions between the approaching path decision and cruise speed adjustment for a robust schedule design that satisfies the needs of solution quality and computation time. The proposed methods in K. K. H. Ng, Chen, and Lee (2020)'s and K. K. H. Ng, Lee, et al. (2020b)'s work attempt to enumerated all the worst-case scenarios in all possible alternative path for determining the solution for robust TTFP at strategic flight approach path decision. Their methods are only applicable in optimising the pre-assigned path decision. In pre-tactical decision, the flight approach paths are usually fixed and ATCOs can make adjustment based on a pre-assigned path decision. The latest ATC condition and the manoeuvring preferences of the ATCOs may limit the possible scenarios. To model the characteristics in ATC pre-tactical decision, we first considered a microscopic view of cruise speed adjustment on deterministic schedule based on the prior work on robust TTFP (K. K. H. Ng, Chen, et al., 2020; K. K. H. Ng, Lee, et al., 2020b; K. K. H. Ng et al., 2017). The alternative path model in the first-stage optimisation problem was built using Directed Acyclic Graph (DAG) (Kam K. H. Ng, Chen, & Lee, 2021; K. K. H. Ng, Lee, et al., 2020b) and the second-stage optimisation problem was used to determine the robustness cost via Monte Carlo simulation. For the detail of the directed acyclic graph in terminal traffic flow modelling, readers may refer to K. K. H. Ng, C. K. Lee, F. T. Chan, C.-H. Chen, and Y. Qin (2020a)'s and Kam K. H. Ng et al. (2021)'s works for the details of alternative path modelling. Second, the SAA approach for stochastic discrete optimisation offered more robust decisions and computational feasibility to estimate the predicted robustness cost of robust TTFP. The algorithm can progressively estimate the true optimal value and provide good analytical solutions for evaluation on numerical studies. Third, ATCOs can determine the desired additional slack time for longitudinal separation minima of approaching flights on the terminal air route, tolerance the level of efficiency loss from the deterministic schedule and balance the delay time and cruise speed adjustment. These three performance measurements will analyse and assist ATCOs to determine a possible combination of the parameters and ensure a certain acceptance level of solution robustness.

1.4. Organisation of the paper

After the introduction of the state-of-the-art ASSP and TTFP from the literature in **Section 1**, **Section 2** explains the microscopic two-stage optimisation framework of robust schedule design for deterministic schedule. The formulation of a nominal model of TTFP and the robust schedule design for TTFP with approaching speed adjustment are presented in this section. **Section 3** illustrates the performance measurement approach for the proposed method. Before presenting the numerical results of the proposed model, **Section 4** provides a small-scale, real-world instance of model explanation to the readers. The case studies and numerical studies are explained in **Section 5**. Finally, **Section 6** presents the concluding remarks and future research direction of the research problem.

2. Robust schedule design for terminal traffic flow problem

Several assumptions should necessarily be made before the construction of the mathematical model for TTFP. First, the set of approach paths have to be fixed within the decision horizon in the model. Some airports may change their approach routes to ensure successive landings due to a change in runway direction relative to the headwind direction. Second, any abnormal operations, such as unappropriated TMA manoeuvring, human error, etc.[1], are omitted. Third, emergency operations, such as precautionary landings, bird strikes and engine failure, are ignored in the model. Fourth, imprecise arrival time on entry waypoints is expected to fall into a stochastic case due to extreme weather conditions, turbulence and the resilience level of systemic and scheduling performance by the ATCOs. We can then build an empirical probabilistic distribution on the uncertain parameter. Fifth, mono-aeronautical holding is considered in this model, by which flights hold in a racetrack pattern with a maximum number of one turn per holding segment. This assumption is practical as very few situations in an airport require several aeronautical holdings in actual operations of the case airport, unless emergency landing, high level of windshear, sea breeze or turbulence on the runway or extreme weather. The meteorological factors on terminal traffic flow model may need to consider the hazard avoidance strategy and will study in the future work.

2.1. Two-stage framework of robust schedule design for terminal traffic flow schedule

We developed a robust schedule design method using a microscopic two-stage optimisation framework for the stochastic optimisation problem of the terminal traffic flow model. The primary aim of this research is to find the estimated outcome of robustness cost with regard to the total flight delay cost and cruise speed adjustment cost on a deterministic schedule. The case airport is adopting enhanced wake turbulence separation (e-WTS) procedures and longitudinal separation minima following by distance-based measurement. Readers may notice that different airports and ATC may adopt time-based flow management and trajectory-based modelling, in which the proposed model may not be applicable to their application scenarios. The general framework of robust schedule design strategy is illustrated in **Fig. 1**. There is a little concern on the schedule adjustment of deterministic schedule in TTFP. We considered a microscopic two-stage optimisation framework suggested by Högdahl, Bohlin, and Fröidh (2019) and Youkyung Hong et al. (2018). In our approach, we considered two types of input parameters for the schedule adjustment, including the realisation of uncertain arrival time at the entry

[1] Inappropriate TMA manoeuvring, human error and operations include collision with obstacles during take-off and landing (CTOL), runway incursions (RI), loss of separation/midair collisions (MAC) and abnormal runway contact. See ICAO – aviation occurrence categories for further information. https://www.icao.int/APAC/Meetings/2012_APRAST/OccurrenceCategoryDefinitions.pdf

waypoints from historical data and a set of user-specific parameters. The first-stage optimisation problem for TTFP $F(\varphi)$ aims to produce an optimal schedule $\overline{\varphi}$ and is regarded as a deterministic schedule in the second-stage optimisation problem $G(\overline{\varphi})$. Solving the $G(\overline{\varphi})$ can be done fastly as the model aims to estimate the outcome of predicted average robustness cost based on a deterministic schedule (predetermined in the first-stage optimisation problem).

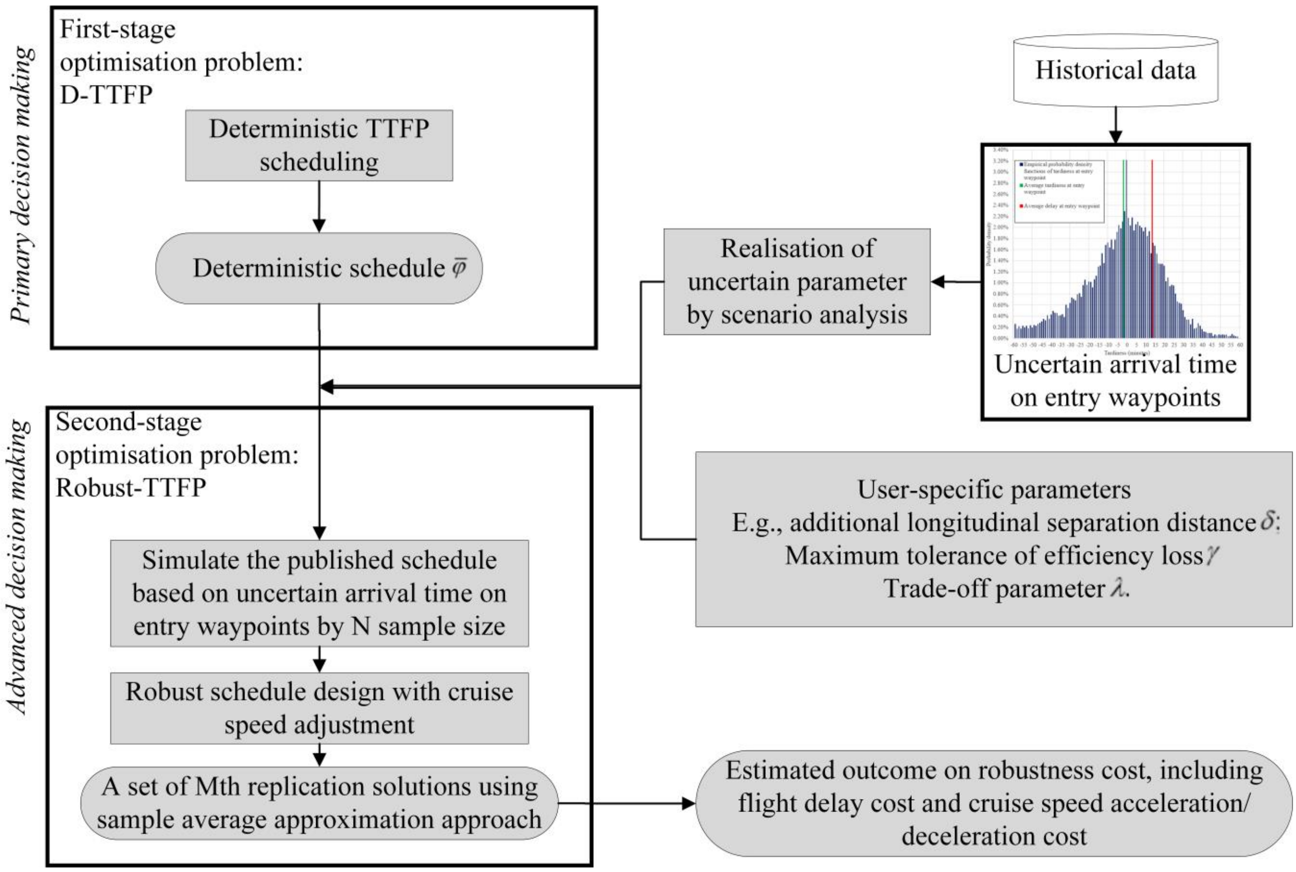

Fig. 1. Robust schedule design for TTFP

The robust schedule design for TTFP $f(\phi)$, namely RSD-TTFP, includes the first-stage D-TTFP and second-stage Robust-TTFP model. Let ϕ be the feasible solution, $\overline{\phi}$ be the optimal solution in the first-stage optimisation problem, namely D-TTFP, and denoted as $F(\phi)$ and T^n be the realisation of the random vector of arrival time at the entry waypoints under the empirical distribution function from historical data. The second-stage optimisation problem with a given deterministic optimal schedule, namely Robust-TTFP, is denoted as $G(\overline{\phi})$. The microscopic two-stage optimisation problem can be formulated as model (1) and (2).

$$min\, f(\phi) = F(\phi) + G(\overline{\phi}) \tag{1}$$

$$s.t.\ X \in \phi(\overline{\varphi}) \tag{2}$$

$H(\overline{\phi})$ is defined as the robustness cost and the expected robustness cost is denoted as $\mathbb{E}\left[\left(H(\overline{\phi})\right)\right]$. The second-stage optimisation problem $G(\overline{\phi})$ is an estimation on robustness cost using an expected function as stated in model (3). We can estimate the expected outcome using the SAA method via Monte-Carlo scenario by enumerating a sufficiently large sample size N on the uncertain parameter in model (4), e.g., the realisation of uncertain arrival time on entry waypoints T^n in our model. In this regard, we can estimate the predicted robustness cost on a terminal traffic flow schedule.

$$G(\overline{\phi}) = \mathbb{E}\left[\left(H(\overline{\phi})\right)\right] \tag{3}$$

$$G(\overline{\phi}) = \frac{1}{N}\sum_{n \in N} H(\overline{\phi}, T^n) \tag{4}$$

ATC has the authority to assign approach routes and request aeronautical holdings to ensure a sufficient longitudinal separation on air routes when controlled flights are under the area control jurisdiction. In standard terminal arrival routes (STARs), approaching flights enter or come close to the TMA (or more specifically, arrive at the terminal airspace sector boundary) by the entry waypoint of the terminal transition routes (TTR), where the entry waypoint is defined as the geographical coordinates on the terminal sector boundary between the air traffic service (ATS) route and navigation route. The purpose of air traffic flow control is to maintain a balance between the airport surface and air route traffic (K. K. H. Ng et al., 2018). The management of air traffic flow control is the key contributor to the overall operational efficiency. Airport surface control, air route segments, aeronautical holding segments and runway resources are the main constraining resources in airport management (K. K. H. Ng et al., 2017). Aeronautical holding requires extra care in terms of the ATC system capacity, foreseen air traffic and anticipated weather disruption near the TMA. Thus, we proposed a terminal traffic flow model to improve the operational efficiency and flexibility of ATC. The number of alternative paths is defined based on the fixed structure of STARs in TMA. Given a fixed structure of STARs and, therefore, all feasible paths can be enumerated as a set of alternative paths. For more details about the alternative paths model, please refer to a recent article (K. K. H. Ng, Lee, et al., 2020b).

The proposed model considers a path planning for each approaching flight within the decision horizon in the TMA as a directed graph $G = (V, E)$ with a set of nodes V and a set of arcs E. Let I be the set of approaching flights. Each flight i has a set of available approaching paths P_i from its entry waypoints to the runway, which is usually predetermined and regulated by ATC rules. For each flight $i \in I$, path $p_i = (u_i^s, \dots, u_i^e)$ describes the path from the entry waypoint to the runways. The entry waypoint is subject to the air route of the departure airport. The origin/destination pair (u_i^s, u_i^e) represents the start (the corresponding entry waypoint) and end (runway) positions. For the sake of simplicity, edge $(u, v) \in E$ indicates the connected nodes. The set of nodes $V_i^{p_i} \subset V$ indicates the collection of the valid waypoints in path p_i, while the set of arc $E_i^{p_i} \subset E$ presents the approach track for flight i to reach the destination using path p_i. Each flight i is assigned a valid path p_i from a set of alternative paths P_i. The set of nodes in the alternative paths model $V_i = \cup_{p \in P_i} V_i^{p_i}$ is the union of a collection of $V_i^{p_i}$ for flight i, while the set of arcs in the alternative paths model $E_i = \cup_{p \in P_i} E_i^{p_i}$ is the union of a collection of $E_i^{p_i}$ for flight i. In this connection, we have $V_j, V_i \in V, E_j, E_i \in E$ in digraph G. **Table 1** presents the notations and decision variables of the model.

Table 1

Notations and decision variables of the nominal model.

D-TTFP	
Sets with indices	Explanation
I	A set of approaching flights in the decision horizon (indexed by i, j)

P_i	A set of alternative paths (indexed by p_i)
V	A vertex set of waypoints in the TMA (indexed by u_i^s, u, v, u_i^e)
E	An edge set of air route in TMA
G	A directed graph consisting of a nonempty vertex set of waypoints V and an edge set of air route E in TMA
Parameters	Explanation
i, j	Flight ID $i, j \in I$
u, v	Transit node $u, v \in V$
u_i^s	The entry waypoint for flight i, $u_i^s \in V$
u_i^e	The approaching runway for flight i, $u_i^e \in V$
p_i	A directed path with a set of waypoints from entry waypoints u_i^s to runway u_i^e for flight $i \in I$, $p_i \in P_i$
T_i	Estimated time of arrival in the terminal control area for flight $i \in I$
$\widehat{\omega}_i$	The upper bound of ground speed on air route in approach phase for flight $i \in I$
$\breve{\omega}_i$	The lower bound of ground speed on air route in approach phase for flight $i \in I$
ω_i	Average ground speed on air route in approach phase for flight $i \in I$
θ_{ji}	Longitudinal separation minima on air route between flights j and $i \in I, j \neq i$
S_{ji}	Separation time on runway between flights j and $i \in I, j \neq i$
M	Large artificial variable
Decision variables	Explanation
X	A solution X is constructed by $\varphi_i^{p_i}$ and z_{jiu}
$\varphi_i^{p_i}$	1, if flight $i \in I$ is assigned to the path $p_i \in P_i$; 0, otherwise
z_{jiu}	1, if flight $j \in I$ is before flight $i \in I, j \neq i$ on node u (not necessary immediately); 0, otherwise
$\tau_{iu}^{p_i}$	The arrival time on waypoint $u \in V$ using path $p_i \in P_i$ for flight $i, \tau_{iu}^{p_i} \geq 0$
$t_{i(u,v)}$	The flight time from waypoints u to v for flight $i \in I$, $t_{i(u,v)} \geq 0$
PTA_i	The preferred time of arrival on runway for flight $i \in I, PTA_i \geq 0$
	Robust-TTFP
Sets with indices	Explanation
N	The sample size (indexed by n)
Parameters	Explanation
n	Scenario
T_i^n	The realised time of arrival in the terminal control area for flight $i \in I$ in scenario $n \in N$
$\underline{\omega}_i$	The minimum speed on air route in approach phase for flight $i \in I$
$\overline{\omega}_i$	The maximum speed on air route in approach phase for flight $i \in I$
δ	Additional buffer distance for longitudinal separation
$\overline{\varphi}_i^{p_i}$	The deterministic schedule from nominal model
F^*	The optimal value of the nominal model
γ	The maximum tolerance of efficiency loss
λ	A user-specific parameter of weighted ratio associate with the total delay cost D_i^n and total penalty cost of cruise speed adjustment P_i^n
Decision variables	Explanation
z_{jiu}^n	1, if flight $j \in I$ is before flight $i \in I, j \neq i$ on node $u \in V$ (not necessary immediately) in scenario $n \in N$; 0, otherwise
τ_{iu}^n	The realised arrival time on waypoint $u \in V$ using path $p_i \in P_i$ for flight $i \in I$ in scenario $n \in N, \tau_{iu}^{p_i} \geq 0$
$t_{i(u,v)}^n$	The realised flight time from waypoints $u \in V$ to $v \in V, u < v$ for flight $i \in I$ in scenario $n \in N$, $t_{i(u,v)} \geq 0$
ETA_i^n	The estimated time of arrival on runway for flight $i \in I$ in scenario $n \in N$, $ETA_i^\sigma \geq 0$
$\alpha_{i(u,v)}^n$	The acceleration time from waypoints $u \in V$ to $v \in V, u < v$ for flight $i \in I$ in scenario $n \in N$, $\alpha_{i(u,v)}^\sigma \geq 0$
$\beta_{i(u,v)}^n$	The deceleration time from waypoints $u \in V$ to $v \in V, u < v$ for flight $i \in I$ in scenario n$\in N$, $\beta_{i(u,v)}^\sigma \geq 0$
D_i^n	The delay time of flight $i \in I$ in scenario n$\in N, D_i^n \geq 0$
P_i^n	The penalty cost of cruise speed acceleration/deceleration of flight $i \in I$ in scenario n$\in N, P_i^n \geq 0$

We introduced a path selection decision variable $\varphi_i^{p_i}$ that determines the approaching path p_i from a set of alternative paths P_i. T_i represents the arrival time at the entry waypoints of flight i. τ_{iu} is a continuous variable to indicate the time instant at which flight i arrives at node u. $t_{i(u,v)}$ is determined by the actual flight time between two entry waypoints $d_{(u,v)}$ and the nominal cruise speed ω_i of flight i, where the nominal cruise speed is a flight-class-dependent variable. For the same type of aircraft (jumbo, heavy, medium or small size types), the average cruise speed of flights is usually a value between $\breve{\omega}_i$ and $\widehat{\omega}_i$. Therefore, the nominal cruise approaching speed without the consideration of acceleration or deceleration is ω_i in $[\breve{\omega}_i, \widehat{\omega}_i]$. We can calculate the $\tau_{iu}^{p_i}$ at each waypoint by considering the travel time $t_{i(u,v)}$ from nodes u to v with the set of predetermined waypoints in the approaching path p_i. In this connection, the waypoint arrival sequence on each node z_{jiu}, which is a binary variable, and the preferred time of arrival PTA_i, which is a continuous variable, can be determined. z_{jiu} is a binary variable to illustrate the arrival sequences on waypoint u for any pair of flights j and i. If flight j is before flight i on waypoint u (not necessary immediately), $z_{jiu} = 1$; otherwise, $z_{jiu} = 0$. PTA_i is a continuous variable in the objective function to calculate the ideal arrival time on runway. Two ATC rules were considered in the model. The longitudinal separation minima θ_{ji} regulate the safe approaching distances on the waypoints between a pair of flights $j, i \in I$, while the final approaching separation time requirement S_{ji} is a buffer time for a pair of flights $j, i \in I$ to accommodate the adverse effect of wake vortex on the runway. A nominal schedule is designed by considering the operational constraints, including path assignment, ideal landing time estimation, cruise speed constraint, arrival sequence, longitude separation constraint (minimum distance separation) and runway separation constraint (minimum time separation).

2.2. Mathematical formulation of D-TTFP

The following explains the constraints and objective function in the D-TTFP:

Alternative paths constraints

$$\sum_{p_i \in P_i} \varphi_i^{p_i} = 1, \forall i \in I \tag{5}$$

$$z_{jiu} + z_{iju} \leq 1, \forall i, j \in I, i < j, \forall u \in V_j \cap V_i \tag{6}$$

$$\varphi_i^{p_i} + \varphi_j^{p_j} \leq z_{jiu} + z_{iju} + 1, \forall i, j \in I, i \neq j, \forall u \in V_j \cap V_i, \forall p_i \in P_i, \forall p_j \in P_j \tag{7}$$

$$\varphi_i^{p_i} \in \{0,1\}, \forall i \in I, \forall p_i \in P_i \tag{8}$$

$$z_{jiu} \in \{0,1\}, \forall j, i \in I, j \neq i, \forall u \in V_j \cap V_i \tag{9}$$

The decision variable $\varphi_i^{p_i}$ is used to determine the selection of an approach path $p_i \in P_i$ for each flight $i \in I$, while z_{jiu} denotes the sequential relationship of flights j and i on waypoint u if both flights pass through the same waypoint. The arrival time at each node u is represented by a continuous decision variable $\tau_{iu}^{p_i}$, which is associated with selected path p_i and its corresponding transit waypoint $u \in V_i^{p_i}$. Constraint set (5) enforces that each flight can only select one path from a set of alternate paths. Constraint set (6) computes the sequence at node u using the binary variable z_{jiu}. Constraint set (7) confirms the sequential relationship of flights j and i at node u, where node u must be a complementary element of V_j and V_i. Constraints (8) and (9) illustrate that $\varphi_i^{p_i}$ and z_{jiu} are binary variables.

Arrival time at entry waypoints and preferred time of arrival on runway

$$\tau_{iu_i^s} \geq T_i \varphi_i^{p_i}, \forall i \in I, \forall p_i \in P_i \quad (10)$$

$$PTA_i = \tau_{iu^e}, \forall i \in I \quad (11)$$

$$\tau_{iu} \geq 0, \forall i \in I, \forall u \in P_i \quad (12)$$

$$PTA_i \geq 0, \forall i \in I \quad (13)$$

The arrival time of flight at the entry waypoint is equal to the time T_i when flight i first appears in TMA is illustrated by Constraint (10). Constraint (11) explained that the ideal time of arrival PTA_i of flight i on the runway equals the arrival time on destination node τ_{iu^e} in the digraph. τ_{iu} and PTA_i are denoted as positive continuous variables by Constraint (12) and (13).

Approaching time from entry waypoint to the runway

$$\tau_{iv} - \tau_{iu} \geq t_{i(u,v)} - M\left(1 - \varphi_i^{p_i}\right), \forall i \in I, \forall p_i \in P_i, \forall (u,v) \in E_i, u < v \quad (14)$$

$$\frac{d_{(u,v)}}{\widehat{\omega}_i} \leq t_{i(u,v)} \leq \frac{d_{(u,v)}}{\breve{\omega}_i}, \forall i \in I, \forall (u,v) \in E_i, u < v \quad (15)$$

$$t_{i(u,v)} \geq 0, \forall i,j \in I, i \neq j, \forall u \in V_j \cap V_i \quad (16)$$

The first arrival time at entry waypoint $\tau_{iu_i^s}$ indicates the start time of approaching. Constraint set (14) calculates the arrival time on the subsequent waypoints, where the waypoints of a path are dependent on the path assignment $\varphi_i^{p_i}$. Therefore, we can compute the time instant on the waypoints in path $p_i = (u_i^s, \dots, u_i^e)$ if ATCOs assigns an approaching path p_i to flight i. We imposed lower and upper bounds of economic cruise speed $\omega_i = [\breve{\omega}_i, \widehat{\omega}_i]$ to determine the travel time on actual distance between waypoints $d_{(u,v)}$. Constraint (15) illustrates that each flight takes $t_{i(u,v)}$ to travel from precedent waypoint u to subsequent waypoint v. Constraint (16) explains that the travel time from waypoints u to v for flight i is a positive continuous variable.

Arrival sequences on waypoints

$$\tau_{iu} - \tau_{ju} \leq M z_{jiu}, \forall i,j \in I, i \neq j, \forall u \in V_j \cap V_i \quad (17)$$

$$\tau_{ju} - \tau_{iu} \leq M z_{iju}, \forall i,j \in I, i \neq j, \forall u \in V_j \cap V_i \quad (18)$$

$$z_{ijv} - z_{iju} \geq \sum_{p_i \in P_i} \varphi_i^{p_i} + \sum_{p_j \in P_j} \varphi_j^{p_j} - 2, \forall j,i \in I, j \neq i, \forall (u,v) \in E_j \cap E_i \quad (19)$$

Regarding the arrival time on each waypoint using path p_i, constraints (17) and (18) explain the bypassing sequence on node u for flight j and i. Constraint (19) describes the overtaking constraints of any pair of flights j and i.

Longitudinal separation constraints (minimum distance separation)

$$\tau_{iu} - \tau_{ju} \geq \frac{\theta_{ji}}{\omega_i} - M\left(1 - z_{jiu}\right), \forall i,j \in I, i \neq j, \forall u \in V_j \cap V_i \quad (20)$$

After determining the bypassing sequence on node u, hard constraint on air route longitudinal separation requirement is modelled by Constraint (20). The arrival time on the node must satisfy the minimum distance separation δ_{ji} for any pair of flights j and i to ensure a safe approaching operation. In order to resolve overtaking constraint of trailing flight, the longitudinal separation time is computed by $\frac{\theta_{ji}}{\overline{\omega_i}}$, where $\overline{\omega_i}$ is the average approaching speed of the trailing flight. **Fig. 2** illustrates the differences between longitudinal separation minima and realised longitudinal separation distance.

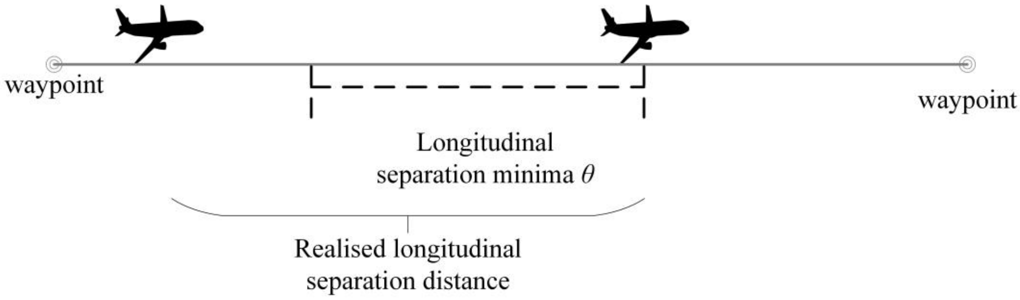

Fig. 2. Illustration of longitudinal separation minima and realised longitudinal separation distance

Final approaching separation constraints (minimum time separation)

$$PTA_i - PTA_j \geq S_{ji} - M\left(1 - z_{jiu_i^e}\right), \forall i,j \in I, i \neq j, \forall u_i^e \in V_j \cap V_i \quad (21)$$

Constraint (21) imposes a minimum separation time to include a sufficient buffer between ideal arrival time PTA_i on a runway for any pair of flights j and i. **Fig. 3** describes the differences between runway separation minima and realised runway separation time.

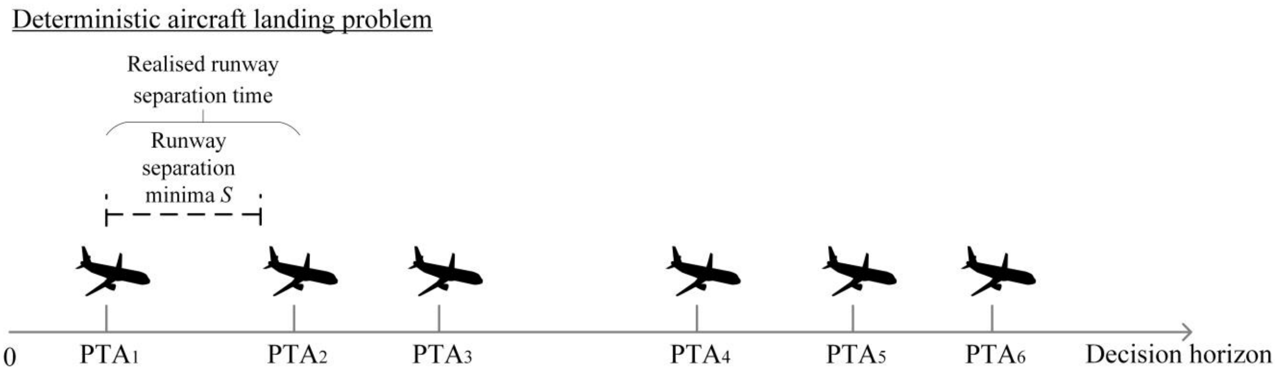

Fig. 3. Schematic diagram of runway separation minima and realised runway separation time

We are interested in determining the ideal arrival time on a runway in the deterministic schedule and capture the flight performance in actual operations. In general, the minimisation of the sum of the preferred times of arrival for all flights, as described in Equation (22) provides a nominal schedule that satisfies the ATC operational requirement in the planning stage. By solving a medium level of instances, the decision from the nominal model can provide a nominal solution to determine the number of aeronautical holdings for particular flights and estimate the preferred time of arrival on runway.

$$F(\varphi) = min \sum_{i \in I} PTA_i \tag{22}$$

$s.t.$ *Constraints* (5) – (21)

2.3. Mathematical modelling of Robust-TTFP

In previous section, we discuss the mathematical modelling for D-TTFP. The optimal schedule $\overline{\phi}$ will pass to the second-stage optimisation problem Robust-TTFP to optimise with the presence of uncertain parameters. For instance, **Fig. 4** illustrates three flights in a system in pre-determined solution in D-TTFP. In actual operations, the arrival time may deviate from the nominal value and subject to uncertain factors. In this regard, it may lead to an infeasible solution of violating longitudinal separation minima, as described as in **Fig. 5**. We will illustrate the manoeuvre procedure of Robust-TTFP in resolving the potential conflict issue in a pre-tactical stage.

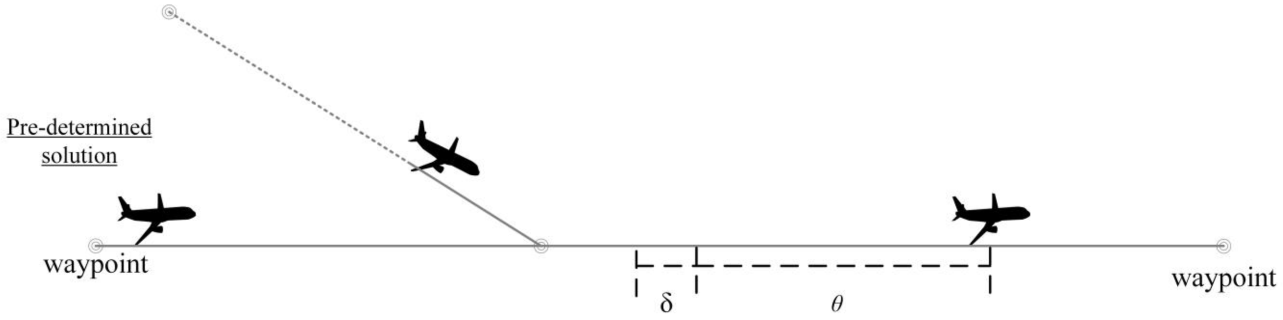

Fig. 4. Pre-determined solution in D-TTFP

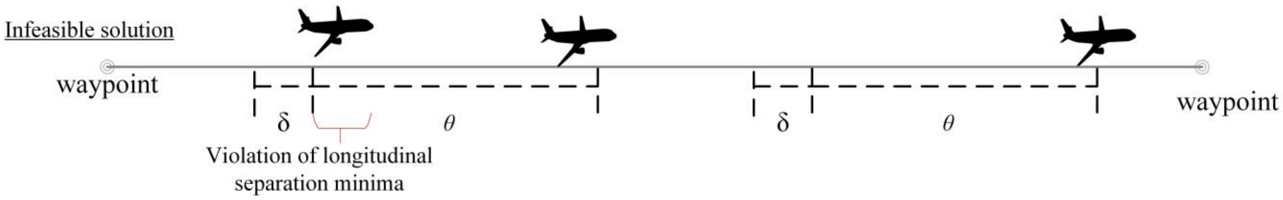

Fig. 5. Infeasible solution in actual operations

In this section, Robust-TTFP was considered as a minor perturbation of arrival time following a probability density function (PDF) at the entry waypoints and approaching speed control. Given a deterministic optimal schedule, a robust schedule design on a microscopic level was introduced to reduce the vulnerability to schedule disruption and impose cruise speed assignment to absorb the delay in ATC. The Robust-TTFP attempted to undertake the consideration of arrival time on entry waypoints uncertainty, while at the same time, controlling the delay propagation and compensating with efficiency loss by cruise speed control.

Compared to the traditional robust optimisation approach, the proposed robust schedule design method is slightly different. In the robust optimisation approach, the decision variables can be an unlimited stretch of the timetable or schedule to accommodate the uncertain parameters. However, in the approaching procedure in ATC, the non-stop process in the TMA is one of the characteristics of TTFP and the adjustment of cruise speed is limited. A zero-efficiency loss of schedule may not be feasible, and the delay cannot be totally absorbed by cruise speed acceleration. The trade-off between cost of cruise speed acceleration/deceleration and efficiency loss to accommodate the air traffic delay is the primary investigation in the model.

The notations and decision variables of Robust-TTFP are listed in **Table 1Error! Reference source not found.**. The mathematical formulation of the model is presented as follows:

We assumed that the delay response of the RSD-TTFP was limited to an optimal deterministic schedule $\overline{\varphi}_i^{p_i}$ that was obtained from the D-TTFP and unable to handle major disruptions, such as unstable weather in the TMA, flight cancellation or landing at a neighbouring airport due to heavy congestion at the destination airport. Roughly speaking, the robust schedule design is a solution that is robust against the en-route traffic delay and controls the cruise speed acceleration/deceleration in the upcoming medium-size level schedule for TTFP. We formulated the robust schedule design as follows:

Uncertain arrival time following a PDF from historical data on entry waypoints

$$\tau_{iu_i^s}^n \geq T_i^n \overline{\varphi}_i^{p_i}, \forall i \in I, \forall n \in N \tag{23}$$

The uncertain arrival time on entry waypoints $\tilde{T}_i$ is considered to be a possible realisation of scenarios, which is a common method of solving stochastic optimisation problems using Monte Carlo simulation. This delay in flight time due to en-route traffic will increase the complexity of the prefect estimation on the arrival time at entry waypoints. Constraint (24) illustrated that the arrival time on entry waypoints $\tau_{iu_i^s}^n$ is greater than or equal to the estimated time of arrival at the entry waypoints of each flight T_i^n in each scenario n.

Approaching sequences on waypoints

$$z_{jiu}^n + z_{iju}^n \leq 1, \forall i, j \in I, i < j, \forall u \in V_j \cap V_i, \forall n \in N \tag{24}$$

$$z_{jiu}^n + z_{iju}^n + 1 \geq \overline{\varphi}_i^{p_i} + \overline{\varphi}_j^{p_j}, \forall i, j \in I, i \neq j, \forall u \in V_j \cap V_i, \forall n \in N \tag{25}$$

Given a planned schedule in the nominal problem, the path assignment and aeronautical holding decision are computed as a planned schedule. Constraint set (24) computes the sequence at node u in scenario n using the binary variable z_{jiu}^n. Constraint (25) illustrates the path assignment and decision variable of bypassing sequence z_{jiu}^n on node u in each scenario n.

Arrival sequences on waypoints

$$\tau_{iu}^n - \tau_{ju}^n \leq M z_{jiu}^n, \forall i, j \in I, i \neq j, \forall u \in V_j \cap V_i, \forall n \in N \tag{26}$$

$$\tau_{ju}^n - \tau_{iu}^n \leq M z_{iju}^n, \forall i, j \in I, i \neq j, \forall u \in V_j \cap V_i, \forall n \in N \tag{27}$$

$$z_{ijv}^n - z_{iju}^n \geq \sum_{p_i \in P_i} \overline{\varphi}_i^{p_i} + \sum_{p_j \in P_j} \overline{\varphi}_j^{p_j} - 2, \forall j, i \in I, j \neq i, \forall (u, v) \in E_j \cap E_i, \forall n \in N \tag{28}$$

Longitudinal separation constraints (separation distance minima)

$$\tau_{iu}^{n} - \tau_{ju}^{n} \geq \frac{\theta_{ji} + \delta}{\omega_i} - M\left(1 - z_{jiu}^{n}\right), \forall i, j \in I, i \neq j, \forall u \in V_j \cap V_i, \forall n \in N \tag{29}$$

The arrival sequences on waypoints and longitudinal separation constraints are explained in Constraints (26–29), which were modified on considering the realisation of scenario σ of Constraints (17–20). In particular, the additional buffer δ is a user-specific slack buffer to enhance the solution robustness. In our proposed approach, the realised longitudinal separation distance must equal to or larger than the flight time considering the longitudinal separation minima θ_{ji} and ATC-specified buffer δ. As shown in **Fig. 6**, the additional buffer can serve as a delay absorption manoeuvre approach to avoid violation of longitudinal separation minima and the possibility of rescheduling.

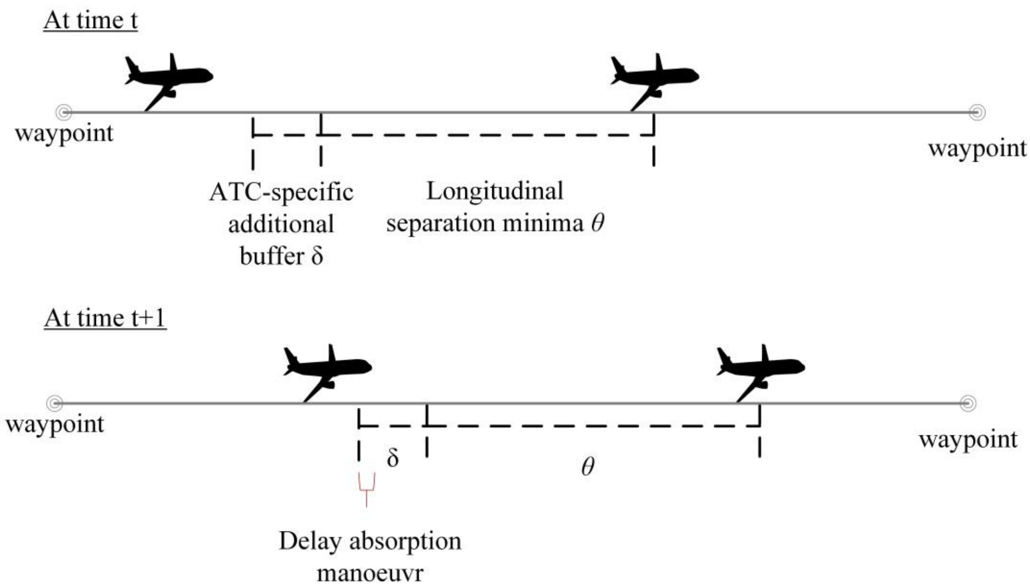

Fig. 6. Schematic diagram of ATCOs-specified buffer on longitudinal separation minima (change to manoeuvre)

Cruise speed acceleration/deceleration

$$\tau_{iv}^{n} - \tau_{iu}^{n} \geq t_{i(u,v)}^{n} - M\left(1 - \overline{\varphi}_{i}^{p_i}\right), \forall i \in I, \forall p_i \in P_i, \forall (u,v) \in E_i, u < v, \forall n \in N \tag{30}$$

$$\frac{d_{(u,v)}}{\overline{\omega}_i} \leq t_{i(u,v)}^{n} \leq \frac{d_{(u,v)}}{\underline{\omega_i}}, \forall i \in I, \forall (u,v) \in E_i, u < v, \forall n \in N \tag{31}$$

$$\tau_{iu}^{n} \geq 0, \forall i \in I, \forall u \in P_i, \forall n \in N \tag{32}$$

The idea of cruise speed acceleration and deceleration is simple. The travel time between waypoints $t_{i(u,v)}^{n}$ in scenario n is computed considering the actual distance between waypoints $d_{(u,v)}$ and the cruise speed. In Constraint (15), we explained that the cruise speed of flight i falls in the range of the average cruise speed $\omega_i = [\breve{\omega}_i, \hat{\omega}_i]$. We further extended the range of the cruise speed by considering its minimal $\underline{\omega_i}$ and maximum cruise speed $\overline{\omega}_i$, so that $\omega_i = [\underline{\omega_i}, \overline{\omega}_i]$ in Constraints (30) and (31). Constraint (32) indicates that τ_{iu}^{n} is a positive continuous variable.

Estimated time of arrival on runway under uncertainty

$$ETA_i^n = \tau^n_{iu_i^e}, \forall i \in I, \forall n \in N \tag{33}$$

$$ETA_i^n - ETA_j^n \geq S_{ji} - M\left(1 - z^n_{jiu_i^e}\right), \forall i,j \in I, i \neq j, \forall n \in N \tag{34}$$

The estimated time of arrival on runway ETA_i^n equals the time on the destination node in scenario n in a digraph by Constraint (33). Constraint (34) enforces that the estimated time of arrival on runway must satisfy the runway separation time regulation S_{ji}.

Efficiency loss

$$\sum_{i \in I} (ETA_i^n) \leq (1+\gamma)F^*, \forall n \in N \tag{35}$$

Let γ be the maximum tolerance of efficiency loss from the nominal schedule and F^* be the optimal value of the nominal problem. One may note that the F^* equals the sum of preferred time of arrival PTA_i in the optimal D-TTFP. The maximum tolerance of efficiency loss is a user-input parameter γ. It is important to understand that it is not necessary to enforce $ETA_i^n \geq PTA_i, \forall n \in N$, as the approaching and landing sequences need not be the same as the nominal solution (but this requirement can be included based on user preferences) after considering the cruise speed acceleration and deceleration. The acceleration and deceleration of approaching may change the sequence of the final approach as flights may enter the joint segments at a different time. The efficiency loss is explained in Equation (35).

Cost of robustness

$$\alpha^n_{i(u,v)} \geq \frac{d_{(u,v)}}{\hat{\omega}_i} - t^n_{i(u,v)}, \forall i \in I, \forall (u,v) \in E_i, u < v, \forall n \in N \tag{36}$$

$$\beta^n_{i(u,v)} \geq t^n_{i(u,v)} - \frac{d_{(u,v)}}{\breve{\omega}_i}, \forall i \in I, \forall (u,v) \in E_i, u < v, \forall n \in N \tag{37}$$

$$\alpha^n_{i(u,v)} \geq 0, \forall i \in I, \forall (u,v) \in E_i, u < v, \forall n \in N \tag{38}$$

$$\beta^n_{i(u,v)} \geq 0, \forall i \in I, \forall (u,v) \in E_i, u < v, \forall n \in N \tag{39}$$

$$D_i^n \geq 0, \forall i \in I, \forall n \in N \tag{40}$$

$$D_i^n \geq ETA_i^n - PTA_i, \forall i \in I, \forall n \in N \tag{41}$$

$$P_i^n \geq \sum_{(u,v) \in E_i\{o,d\}} \left(\alpha^n_{i(u,v)} + \beta^n_{i(u,v)}\right), \forall (u,v) \in E_i, u < v \tag{42}$$

The realised travel time between waypoints $t^n_{i(u,v)}$ is a continuous variable. We measure the acceleration and deceleration of cruise speed in a unit of time. $\alpha^n_{i(u,v)}$ and $\beta^n_{i(u,v)}$ are the realised penalty cost (per time unit) of acceleration and deceleration from waypoint u to waypoint v for flight i in scenario n. The sum of the penalty cost of acceleration and deceleration is defined as the cost of robustness. Constraints (36) and (37) compute the penalty cost, while Constraints (38) and (39) indicate that $\alpha^n_{i(u,v)}$ and $\beta^n_{i(u,v)}$ are positive continuous variables. Constraints (40) and (41) compute the delay time from PTA_i in scenario n. Given the scenario as shown in **Fig. 5**, ATC can communicate with pilots and execute speed acceleration or deceleration, as shown in **Fig. 7** and **Fig. 8**, respectively, to avoid the violation of longitudinal separation minima.

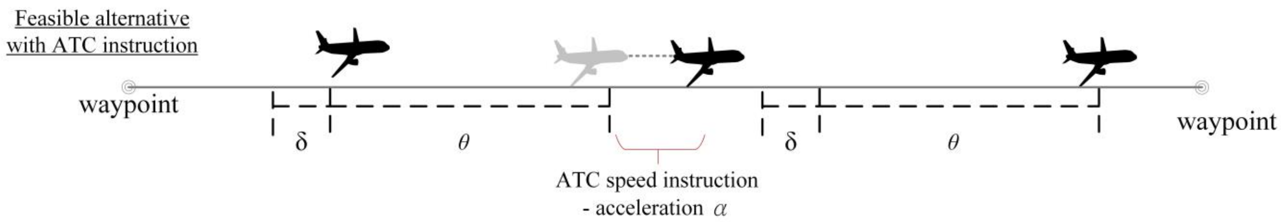

Fig. 7. Feasible alternative with ATCOs' speed instruction of acceleration

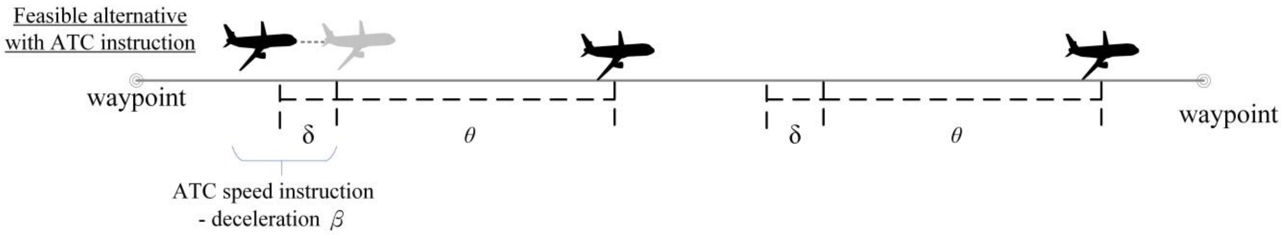

Fig. 8. Feasible alternative with ATCOs' speed instruction of deceleration

Constraint (42) indicates the penalty cost of cruise speed acceleration/deceleration from the entry waypoints to the runway. **Fig. 9** presents the induced additional flight time penalty in one alternative under the impact of empirical arrival delay on entry waypoint.

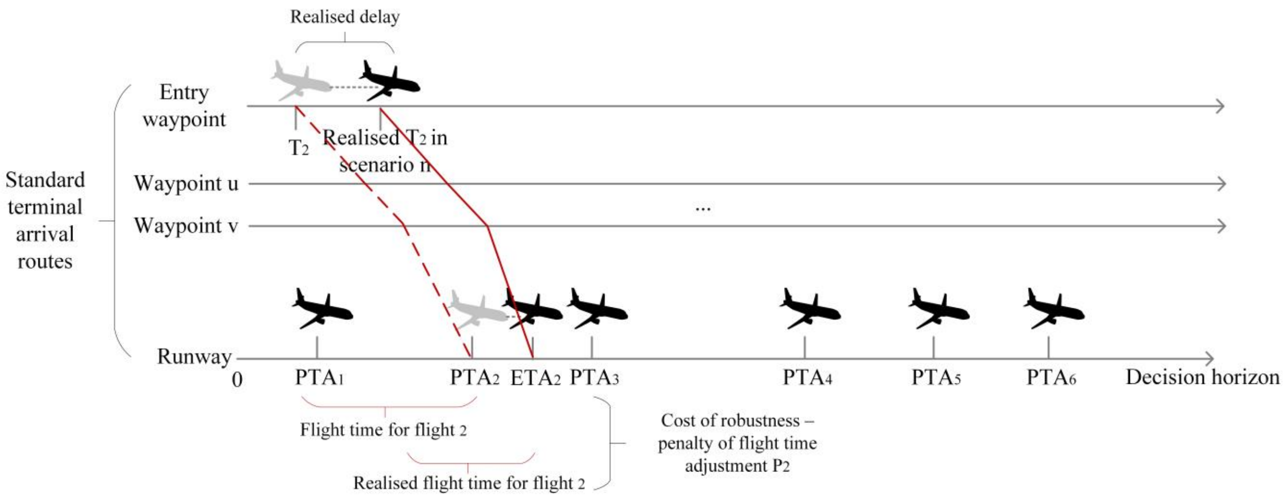

Fig. 9. Schematic diagram of penalty cost of increase in flight time in one of the alternatives

The complete formulation of the Robust-TTFP is shown as follow:

$$min\ G(\overline{\varphi}) = \frac{1}{N}\sum_{n\in N} H(\overline{\varphi}, T^n) = \frac{1}{N}[\sum_{i\in I}\sum_{n\in N}(\lambda D_i^n + (1-\lambda)P_i^n)] \tag{43}$$

$s.t.$ Constraints (23) – (41)

The objective function of robust-TTFP is to minimise the weighted function of total delay cost and total penalty cost, namely the cost of robustness, in Equation (43), where the total delay cost is the sum of the delay time D_i^n of each scenario n and the total penalty cost of cruise speed acceleration/deceleration is the sum of time of cruise speed acceleration/deceleration of each scenario n. The ratio of λ is a user-specific parameter that indicates the weight ratio between the total delay cost and total penalty cost of cruise speed acceleration/deceleration, where $\lambda = [0.0,1.0]$. **Fig. 10** illustrates the possible impact of realised delay on estimated time of arrival ETA_i^n and predicted time of arrival on runway PTA_i in one of the alternatives.

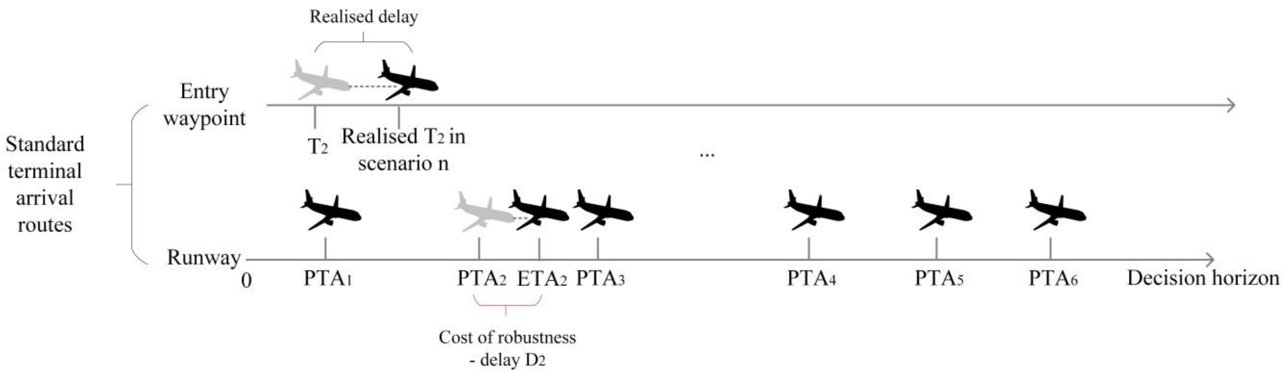

Fig. 10. Schematic diagram of arrival delay on runway and the cost of delay time in one of the alternatives

3. Performance measurements

In the robust schedule design for TTFP with cruise speed adjustment, we considered several performance measurements to indicate the performance trade-off in hedging exogenous uncertainty on arrival time at entry waypoints. The arrival time on entry waypoints $\tilde{T}_i$ follows a PDF from historical data. It is unlikely that the estimated arrival time at the entry waypoints is equal to the actual one as the en-route uncertainty is subject to en-route traffic, flight time from origin and destination airports and weather. Given the uncertain nature of the arrival time at the entry waypoints, a robust schedule design favours delay compensation. **Fig. 11** presents the empirical distribution function of arrival lateness at entry waypoints. Lateness is defined as a positive or negative deviation from the nominal arrival time at entry waypoint, while delay is defined as zero or positive deviation from the nominal arrival time at entry waypoint. The data was obtained by a licensed Application Programming Interface (API) from *FlightGlobal*, and a total of 14668 arrival records were obtained in April 2018. It is worth noting that Monday and Sunday are having more air traffic movements, and instances with high traffic scenarios shall be separately trained as a second model. The research method for normal and high traffic scenarios are more or less the same. Therefore, the analysis of the high traffic scenarios is omitted in this work. By filtering flight on Monday and Sunday only and the flight is located in hours with 11 air traffic movements or above, only 3889 flight records are valid. The uncertain arrival time at the entry waypoint is a time value that a reference arrival time on entry waypoint provided by the pilot for ATCOs to the prior schedule and the actual one. Note that, in our preliminary analysis, the differences of PDF between waypoints were minimal. The average lateness at entry waypoints was -3.99 minutes and the average delay at entry waypoints was 13.98 minutes.

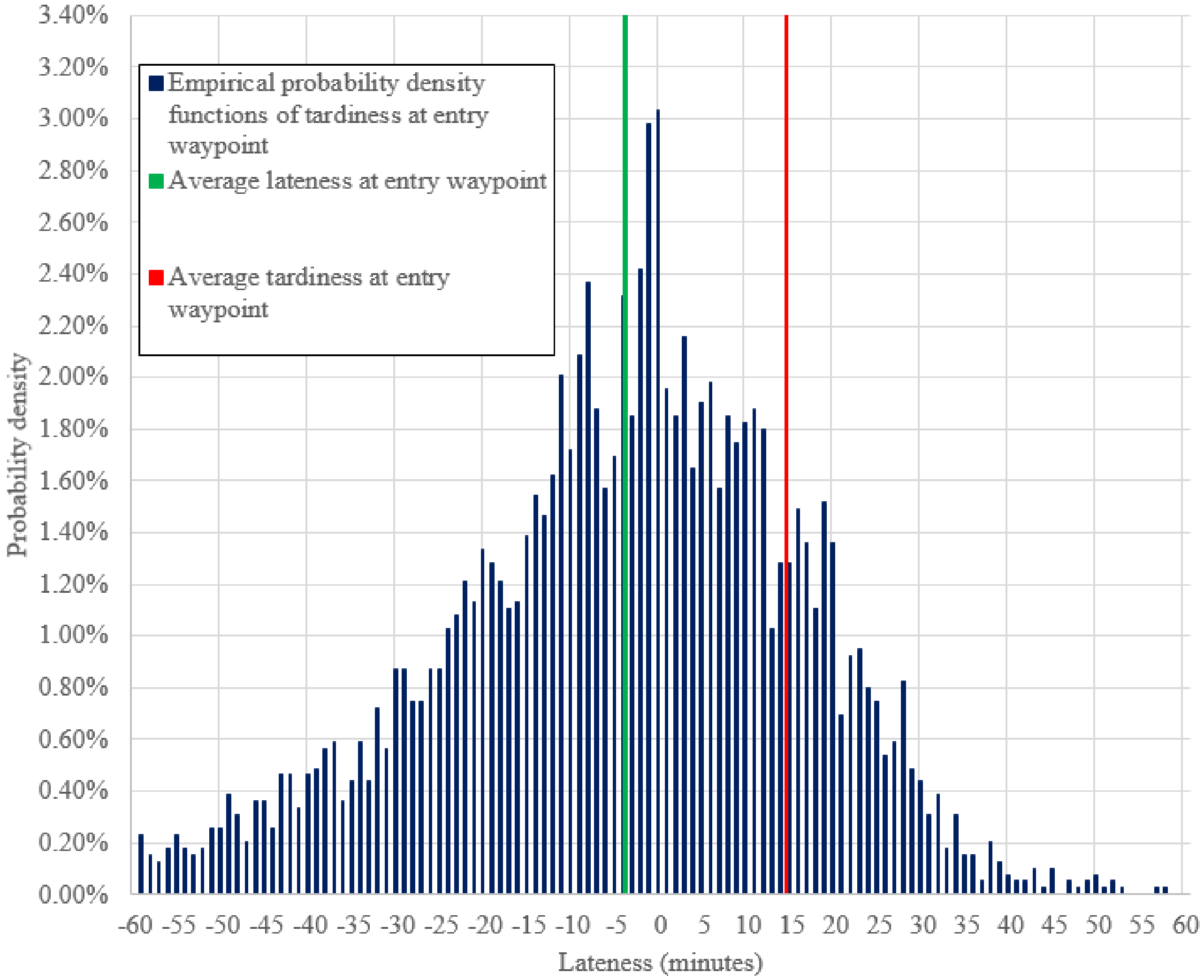

Fig. 11. Empirical distribution function of arrival lateness at entry waypoints.

(For interpretation of the references to colour in the text, the reader is referred to the web version of this article.)

3.1. Performance bound and estimated optimality gap on sample average approximation

As mentioned in Constraint (23) and Objective function (43) of the Robust-TTFP, the arrival time at entry waypoint for each flight in each scenario is denoted as T_i^n, where T_i^n is the value after adding a value generated from empirical PDF from **Fig. 11**. It is worth noting that the computation time with a very large sample size N will increase exponential for NP-hard problem (K. K. H. Ng, Lee, et al., 2020b; K. K. H. Ng et al., 2018; K. K. H. Ng et al., 2017). The true optimal value can be obtained when $N \rightarrow \infty$. Intuitively, solving such stochastic optimisation problem is computationally intractable. SAA offers high quality solutions with the consideration of statistical performance bound and can yield a solution that satisfies the computational needs of the practitioners (Kleywegt, Shapiro, & Homem-de-Mello, 2002). Various engineering applications, including robust liner shipping services, supply chain networks with disruption and stochastic personnel assignment, have adopted SAA or variances of SAA to solve the stochastic optimisation problem (Xiaojun Chen, Shapiro, & Sun, 2019; Li & Zhang, 2018; Pour, Naji-Azimi, & Salari, 2017; Singham, 2019; Wang & Meng, 2012). SAA is still a promising research area for solving the stochastic optimisation problem with Monte Carlo simulation (Högdahl et al., 2019). The pseudo code of the SAA approach is stated in **Algorithm 1**.

Algorithm 1.

A sample average approximation method to solve the proposed model

```
Set the number of replications M, sample size N, a set of additional longitudinal separation minima Ω, a set of maximum tolerance of efficiency loss Γ, a set of trade-off parameters Λ.
Solve the first-stage optimisation problem and obtain the optimal deterministic schedule φ̄
Foreach λ in Λ
    Foreach γ in Γ
        Foreach δ in Δ
        Set m = 0
        While m ≤ M do
            Simulate the optimal deterministic schedule φ̄ and generate a set of uncertain arrival time on entry
          waypoints for all flights (N scenarios) based on the empirical probabilistic distribution from historical
          data
            Solve the m^th second-stage optimisation problem with N sample size in Equation (47)
            Record the objective value of the m^th second-stage optimisation problem with N sample size as υ_N^m
            m = m + 1
            If all the replications of second-stage optimisation problem are optimal or feasible
            Then compute the estimated average robustness cost ῡ_N^M in Equation (46)
        End
    End
End
Map the solutions
```

Monte Carlo simulation solves stochastic optimisation by generating a sufficiently large sample size N' to estimate the outcome of an expected value of an objective function $G_{N'}(\overline{\varphi})$, as stated in Equation (44). $G_{N'}(\overline{\varphi})$ is an unbiased estimator of $G(\overline{\varphi})$ based on a sample size N'. It includes a set of arrival time on entry waypoint for all the flights in each scenario by realising the random vector $\boldsymbol{T}$, i.e. $T^1, T^2, \ldots, T^{N'}$, which is an independently and identically distributed (IID) random sample with the size of N'. Let υ^* be the true optimal value; the optimality gap can be estimated by Equation (45).

$$G_{N'}(\overline{\varphi}) := \frac{1}{N'} \sum_{n \in N'} H(\overline{\varphi}, T^n) \tag{44}$$

$$\theta = G_{N'}(\overline{\varphi}) - \upsilon^* \tag{45}$$

The idea behind using SAA algorithm is to perform replication on $G(\overline{\varphi})$ and approximately estimate the objective value with enough information about the solution. Let υ_N^m be the optimal objective value of m^{th} SAA replication. One can estimate υ^* by M replication of SAA method υ_N^m using Equation (46). Note that the $\mathbb{E}[\overline{\upsilon}_N^M]$ is an unbiased estimator of $\mathbb{E}[\upsilon_N]$. Given that $N < N'$, solving the $G_N(\overline{\varphi})$ is faster with the realisation of random vector $\boldsymbol{T}$, i.e. $T^1, T^2, \ldots, T^N$ of N IID sample by Equation (47).

$$\overline{\upsilon}_N^M := \frac{1}{M} \sum_{m \in M} \upsilon_N^m \tag{46}$$

$$\upsilon_N^m = \frac{1}{N} \sum_{n \in N} H(\overline{\varphi}, T^n) \tag{47}$$

The optimality gap of $G(\overline{\varphi}) - \upsilon^*$ can be estimated by the expected value of $G_{N'}(\overline{\varphi}) - \overline{\upsilon}_N^M$ to their counterparts from the original problem as explained in Equation (48). One can increase the sample size N or reduce N' to achieve a high degree of convergence rate. Furthermore, the decision of sample size N is also associated with the computational requirement from users. Regarding the proof and the algorithm structure could be found in Kleywegt et al. (2002).

$$\mathbb{E}\left[G_{N'}(\overline{\varphi}) - \overline{v}_N^M\right] = G(\overline{\varphi}) - \mathbb{E}[v_N] \geq G(\overline{\varphi}) - v^* \quad (48)$$

3.2. Compensation of solution robustness and operational efficiency

Since the RSD-TTFP model includes several limitations of resource constraints, the model does not have the property of unlimited stretch of the approaching schedule to recover from delays. The proposed model attempts to evaluate the performance of absorbing disturbance by delaying the flight arrival time or adjusting the cruise speed. One may note that this model has not attempted to tackle any major disruption but minor delays as stated in **Fig. 11**. The idea of RSD-TTFP is similar to the idea of light robustness approach, which attempts to maximise the level of protection from the uncertainty outcome and consider the flexible threshold of optimal solution from the D-TTFP schedule (Fischetti, Salvagnin, & Zanette, 2009; Lusby, Larsen, & Bull, 2018; Wee et al., 2018). Therefore, minor delay is the main focus of this model.

3.2.1. Maximum tolerance of efficiency loss from the nominal schedule

The efficiency loss from the nominal schedule is explained in Constraint (35). The preferred time of arrival on runway PTA_i is calculated by the nominal model. The optimal value from the nominal model is denoted as F^*. The maximum tolerance of efficiency loss γ equals or is larger than one. γ is included in the model to provide a restriction on the tolerance of efficiency loss from the optimal value of nominal schedule (Cacchiani & Toth, 2012). When γ is equal to 1, the sum of estimated time of arrival on runway ETA_i^n in each scenario is strictly equal to F^*. When γ is close to 1, the solution tends to have more flights speed up to accommodate the effect of delay. The solution will have a higher level of tolerance for landing delay with larger γ value. The trade-off parameter (namely, efficiency loss) γ is an input of a maximum allowance of percentage increase of F^*. Greater value of $(1+\gamma)F^*$ implies a lower penalty cost of cruise speed adjustment but with a larger sum of estimated time of arrival on runway. Cruise speed acceleration may reduce the estimated time of arrival on runway but the speed up cost contributes to the penalty cost. This trade-off parameter is a user-specific parameter regarding their tolerance of efficiency loss by γ. In our analysis, we evaluate γ in a different value by an incremental increase of 0.1%. We could then map the efficiency loss and penalty cost of cruise speed acceleration/deceleration.

3.2.2. Trade-off between total delay cost and total penalty cost of cruise speed adjustment

The trade-off between the total delay cost D_i^n and total penalty cost of cruise speed adjustment P_i^n is formulated by a convex combination using λ, where $\lambda = [0,1]$. The model is sensitive to delay landing time when $\lambda = 1$ or vice versa.

3.2.3. Robust schedule design with operational safety

We considered an additional buffer for longitudinal separation δ (in nautical miles) by ATCOs in Constraint (29), which is a user-specific value. An additional buffer for longitudinal separation minima can add a certain level of solution robustness with the presence of slack time δ. We could also evaluate the maximum permitted slack time of feasible region of robust schedule design for TTFP as a reference to ATCOs.

4. Small-scale real-world instance demonstration

For the purpose of model explanation, we solved a small-scale, real-world instance on 22nd April 2018 and presented the numerical results graphically. We considered a set of flights with $|I| = 5$ that arrived on the waypoints from 00:00am to 01:00am. The entry waypoints of the flights were different except for flights 4 and 5. All the flights joined at a merge point at GUAVA or LIMES waypoints as shown in **Fig. 12** (detailed waypoints connection is shown in **Fig. 15**). The optimal solution for approaching the waypoints of each flight was obtained by solving the first-stage optimisation problem $F(\varphi)$, and the graphical timetable of the D-TTFP schedule is presented in **Fig. 13**.

We generated four scenarios by realising the random vector $\boldsymbol{T}$, i.e., $T^1, T^2, \dots, T^4$ with regard to the empirical PDF, as stated in **Fig. 11**, and passed the deterministic schedule to the second-stage optimisation problem $G(\overline{\varphi})$. The trade-off parameter λ, maximum tolerance of efficiency loss γ and the slack time on longitudinal separation minima δ are set to be 0.5, 3.0 and 0.0, respectively. The optimal result of robust TTFP with cruise speed adjustment is presented in **Table 2**. $H(\overline{\varphi}, T^n)$ indicates the optimal value in scenario s. The optimal value $H(\overline{\varphi}, T^n)$ in scenario 2 equals to zero, the weighted total delay cost D_I^2 and total penalty cost P_I^2 are zero and no extra delay cost or ground speed adjustment existed. In other words, the uncertain arrival time on entry waypoints in scenario 2 does not affect the overall solution. The set of total delay cost D_I^n and total penalty cost P_I^n indicates that associated cost to each flight in this instance. Given a sample size of 4 in this small-scale real-world instance, the expected robustness cost $G(\overline{\varphi})$ equals to 921.14. We can estimate the possible outcomes of uncertain arrival time on entry waypoints via SAA algorithms and help ATCOs to determine the possible manoeuvring approach to the pilot when the uncertain arrival time on entry waypoints for flights is realised. Readers can refer to one of the optimal timetable schedule scenarios in **Fig. 14**. Difference in slope from the deterministic schedule indicates the acceleration of flights. Each time unit was accumulated as cost of speed adjustment P_i^n when the acceleration speed existed or was below the range of ground speed, as stated in Constraints (36) and (37). The delay cost was calculated by the difference of estimated time of arrival ETA_i^n from the preferred time of arrival PTA_i, as stated in Constraint (41). The robustness cost $H(\overline{\varphi}, T^n)$ was a convex combination of D_i^n and P_i^n with a trade-off parameter λ. The optimal value $G(\overline{\varphi})$ was an average value of $H(\overline{\varphi}, T^n)$ with sample size N.

Table 2

Optimal results of robust TTFP with approaching speed control solving a small-scale real-world instance

$G(\overline{\varphi})$	n	$H(\overline{\varphi}, T^n)$	D_I^n	P_I^n
921.14	1	796.09	{0,339.65,788.78,0,0,0}	{13.34,133.56,316.86,0,0,0}
	2	0	{0,0,0,0,0,0}	{0,0,0,0,0,0}
	3	1499.24	{0,339.65,0,1443.55,925.38,0}	{0,133.56,0,102.29,54.06,0}
	4	1389.22	{0,39.65,0,963.55,0,1211.48}	{13.34,133.56,0,102.29,0,314.57}

$\lambda = 0.5, \gamma = 3.0, \ \delta = 0$

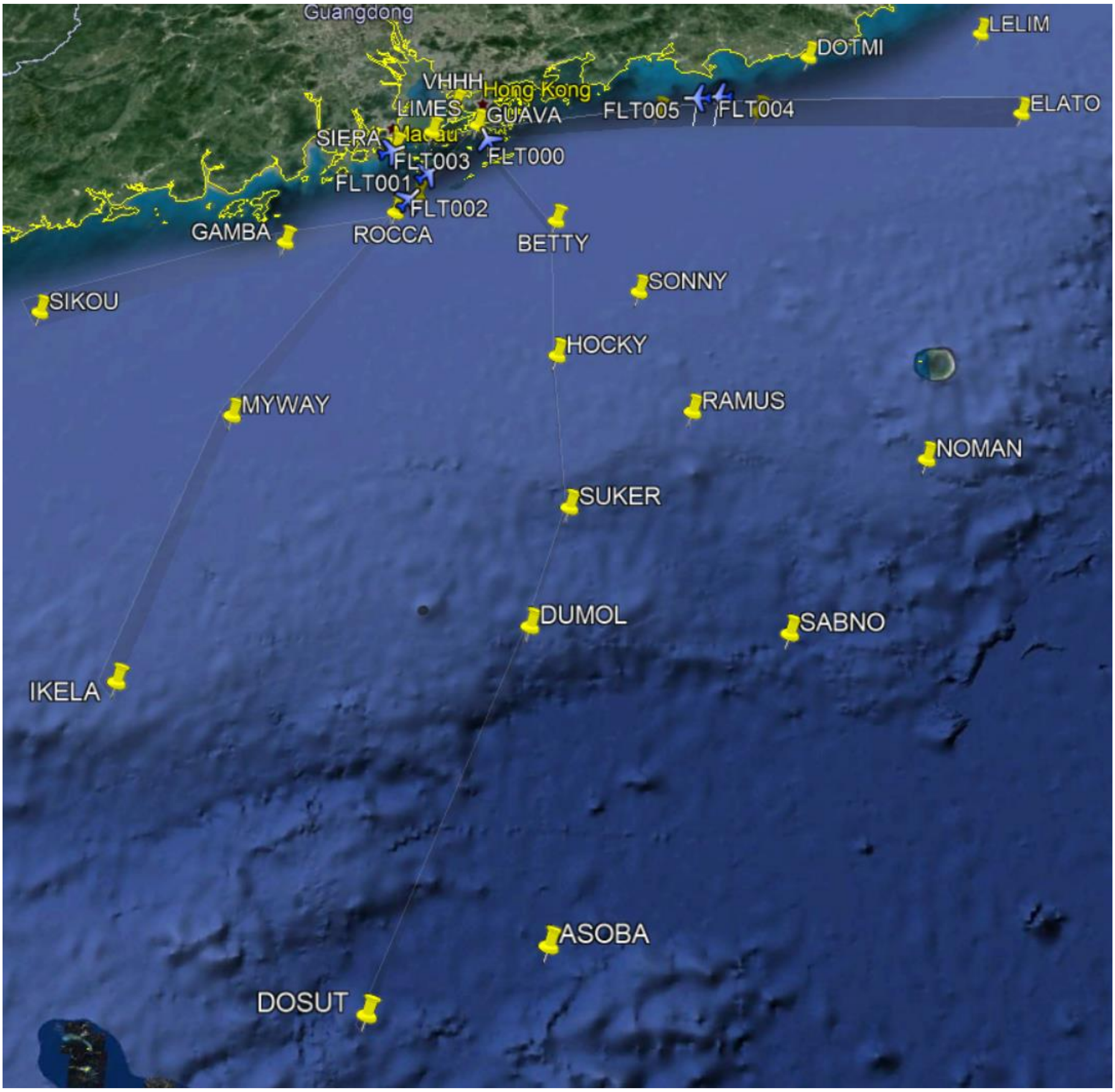

Fig. 12. Optimal path assignment of nominal model solving small scale real-world instance at the timestamp of 01:10:53 powered by Google Earth

(For interpretation of the references to colour in the text, the reader is referred to the web version of this article.)

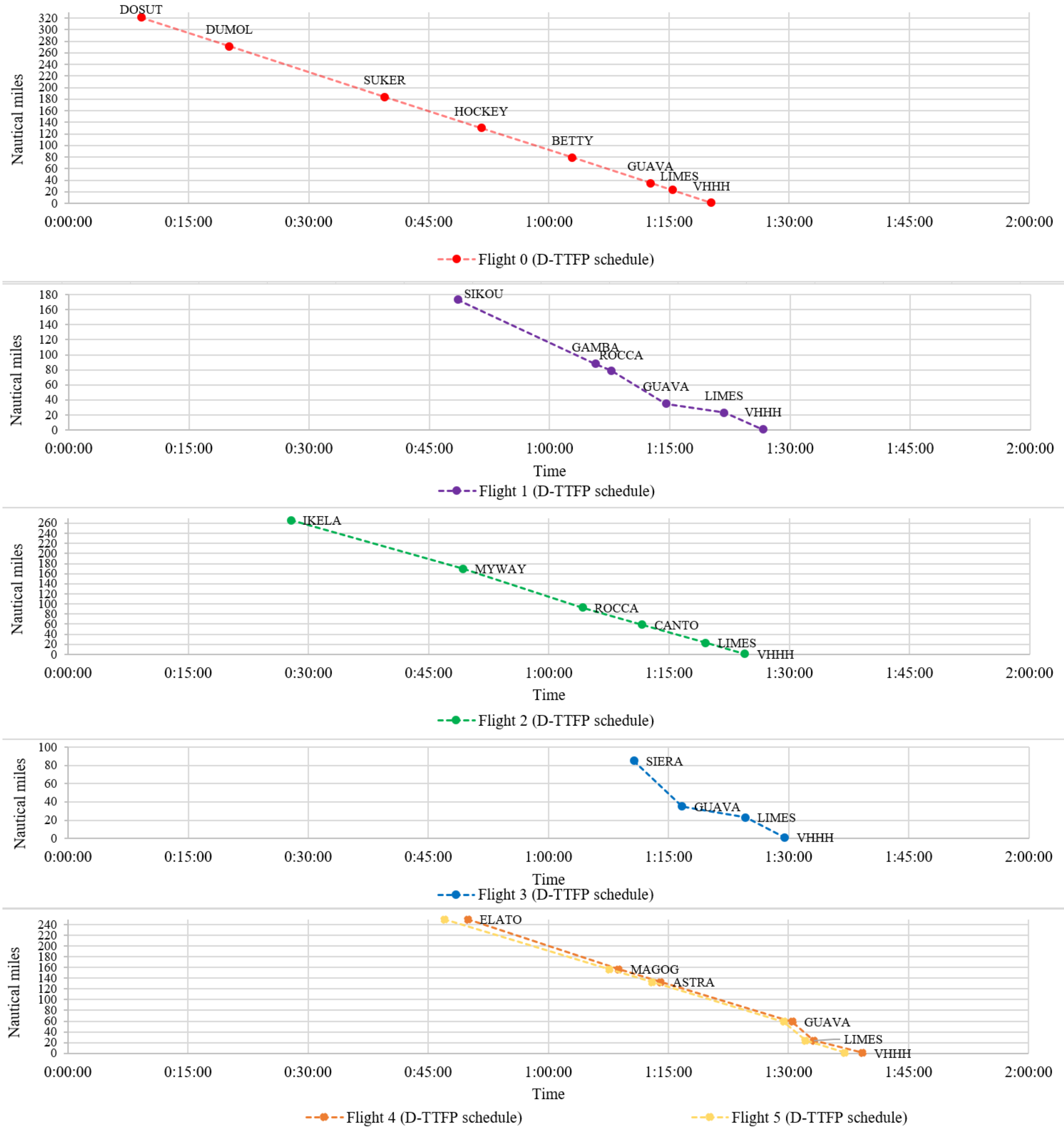

Fig. 13. Graphical timetable representation of optimal solution for nominal TTFP.

(For interpretation of the references to colour in the text, the reader is referred to the web version of this article.)

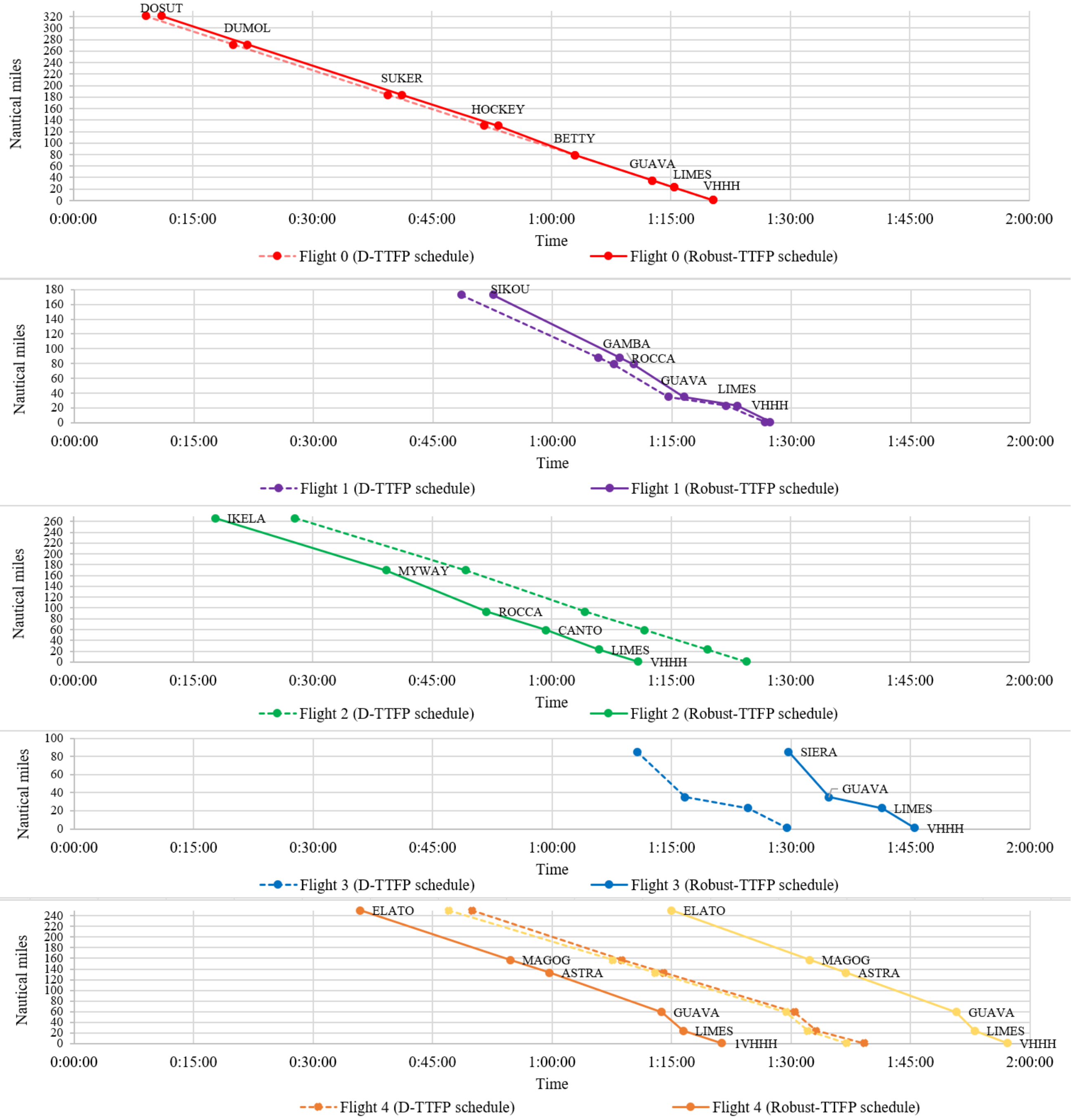

Fig. 14. Optimal solution of cruise speed adjustment under uncertain arrival time on entry waypoint (one of the scenarios)

(For interpretation of the references to colour in the text, the reader is referred to the web version of this article.)

5. Computational results

5.1. Description of the case airport

One set of real-world instances was considered for the robust schedule design for TTFP. We aimed at investigating the performance of solution robustness and the efficiency loss using real-life scenarios. Therefore, we obtained several medium-sized instances from real-world scenarios on 22nd April 2018 at The Hong Kong International Airport (HKIA). **Fig. 15** presents the STARs and geographical positions of the holding circles with actual distances between waypoints in the area control of HKIA. As the length of the holding pattern was sufficient to tackle the conflict situation of the air route setting at the HKIA, we assumed that a mono-aeronautical holding pattern was imposed (Artiouchine et al., 2008). In accordance with the assumption and the instance of the environmental setting, 10 entry waypoints and 26 alternative paths were constructed in our model. Reader may refer to the STARs map in K. K. H. Ng, Lee, et al. (2020b).

A total of 5 instances were extracted from real life scenarios in the evaluation of the model. We considered a medium size of instances as we were concerned about the impact of delay in ATC on the subsequent ATC schedule and the near real-time control of cruise speed of the approaching flights. We first separated the real data on 22nd April 2018 at half-hour intervals and extracted those instances with the number of flights that were more than 10. For each case with the same number of flights, we randomly picked four instances at most for evaluation to avoid lengthy computational analysis. The instance ID was represented by two digits (the value of the hour) and one alphabet (First half an hour by "F" or second by "S"). The longitudinal separation minima (in nautical miles) and runway separation time matrix are referred to the data in (K. K. H. Ng, Lee, et al., 2020b) and (Balakrishnan & Chandran, 2010), respectively. The minimum and maximum of approaching speed for small-size, medium-size and large-size flights are [240,320], [230, 320] and [210, 320], respectively. The range of economic approach speed for small-size, medium-size and large-size flights can be found in K. K. H. Ng, Lee, et al. (2020b). **Table 3** provides a short summary of the real-life instances. The computation was performed with *Intel® NUC 10* the configuration of *Intel Core i9-10900KTi @ 3.70GHz 3.70GHz CPU* and *128.0GB RAM* under *Windows 10 Enterprise 64-bit* operating system. The algorithm was coded using *C# .NET framework* with *Microsoft Visual Studio 2017* and *IBM ILOG CPLEX optimisation Studio 12.8.0*.

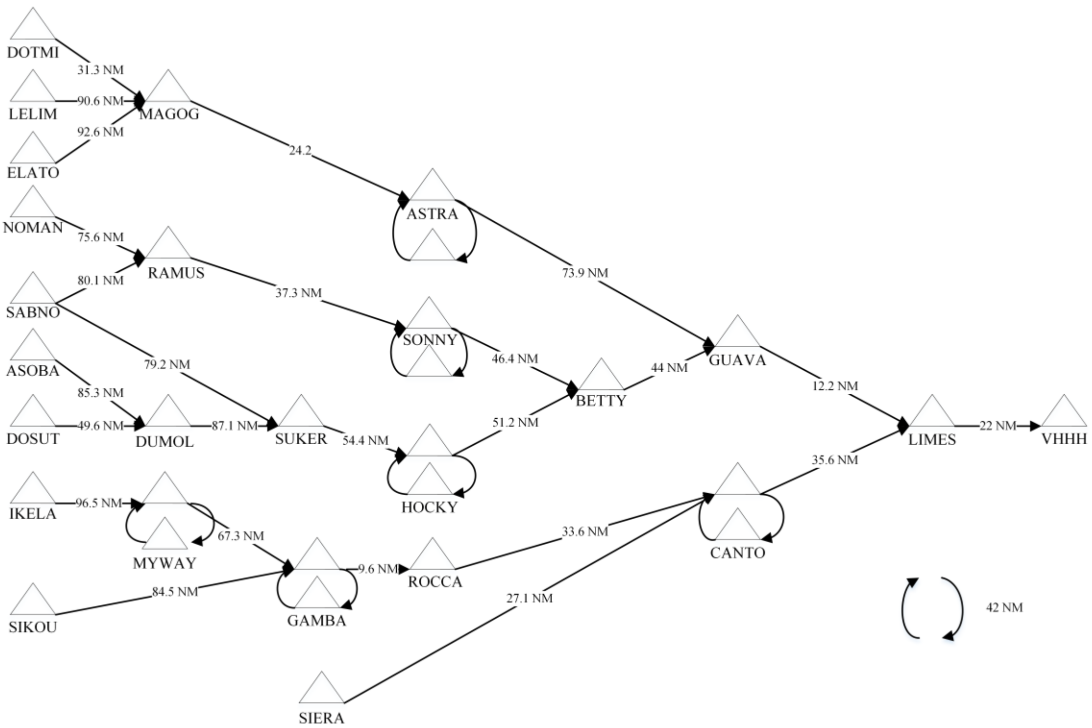

Fig. 15. The schematic graph of the air route network in the terminal manoeuvring area of the case airport.

Table 3

The description of the test instances of flight data on 22nd Apr 2018

ID	$\lvert I \rvert$	Distribution of flight sizes {SSF, MSF, LSF}	Distribution of arrival flights from ten entry waypoints	T_i
08-S	11	{4, 6, 1}	{0, 0, 3, 6, 0, 0, 0, 0, 1, 1}	{7:30, 7:30, 7:41, 7:40, 7:45, 7:51, 7:59, 7:56, 7:52, 7:56, 8:31}
12-F	13	{7, 3, 3}	{1, 1, 6, 1, 0, 0, 1, 0, 2, 1}	{11:10, 11:05, 11:08, 11:29, 11:26, 11:14, 11:20, 11:23, 11:21, 11:59, 11:02, 11:26, 11:33}
12-S	13	{5, 3, 5}	{0, 0, 10, 0, 0, 1, 0, 0, 0, 2}	{11:35, 11:00, 12:08, 11:34, 11:36, 11:45, 12:18, 11:43, 11:50, 11:59, 11:56, 11:57, 11:59}
10-S	15	{9, 3, 3}	{2, 1, 2, 1, 0, 0, 0, 0, 1, 8}	{10:06, 10:08, 9:39, 9:36, 9:35, 10:12, 10:16, 9:57, 9:43, 10:05, 10:06, 10:23, 10:25, 10:30, 10:30}
15-S	16	{9, 4, 3}	{2, 3, 6, 0, 0, 1, 0, 0, 0, 4}	{14:36, 14:37, 15:07, 15:09, 14:38, 14:58, 14:46, 14:49, 14:47, 15:02, 15:28, 14:58, 14:24, 15:30, 15:03}

SSF: Small size flight; MSF: Medium size flight; LSF: Large size flight. Ten entry waypoints: {DOTMI, LELIM, ELATO, NOMAN, SABNO, ASOBA, DOSUT, IKELA, SIKOU, SIERA}

5.2. Numerical study on performance bound, estimated optimality gap and computation time

In this section, we attempted to evaluate the best combination of sample size N and replication M using SAA framework. We randomly picked two relatively large size instances, 12-F and 15-S instances, to study the combination of sample size and replication regarding the quality of performance bound, estimated optimality gap and computation time. The initial setting of the SAA algorithm was $\lambda = 0.5, \gamma = 3.0,\ \delta = 0$. Each instance was a 30-minute arrival interval at entry waypoints and the computation time of RSD-TTFP was suggested to be less than 30 minutes. Intuitively, SAA aims to estimate a solution for a stochastic discrete optimisation problem using Monte Carlo simulation. The quality of estimation of the true optimal value is associated with the variation of the optimal values with a sufficient sample size N and replication M. A larger sample size N implies a better estimation of true optimal value $\overline{v}_N^M$ but which is computationally expensive for NP-hard problem, while an increase in replication M provides more data point to map the average performance of v_N^m with a linear increase in computational time. Less variation of v_N^m indicates a better estimation with sample size N, while replication M is determined by sufficient estimation on v_N^m. In this connection, the determination of sample size N is a problem specified parameter and replication M can be a referenced or user-specified parameter. Therefore, we followed the suggestion from the method by Long, Lee, and Chew (2012) to evaluate the replication M with 10, 20 and 30 and determine the sample size N by solving the proposed stochastic optimisation problem.

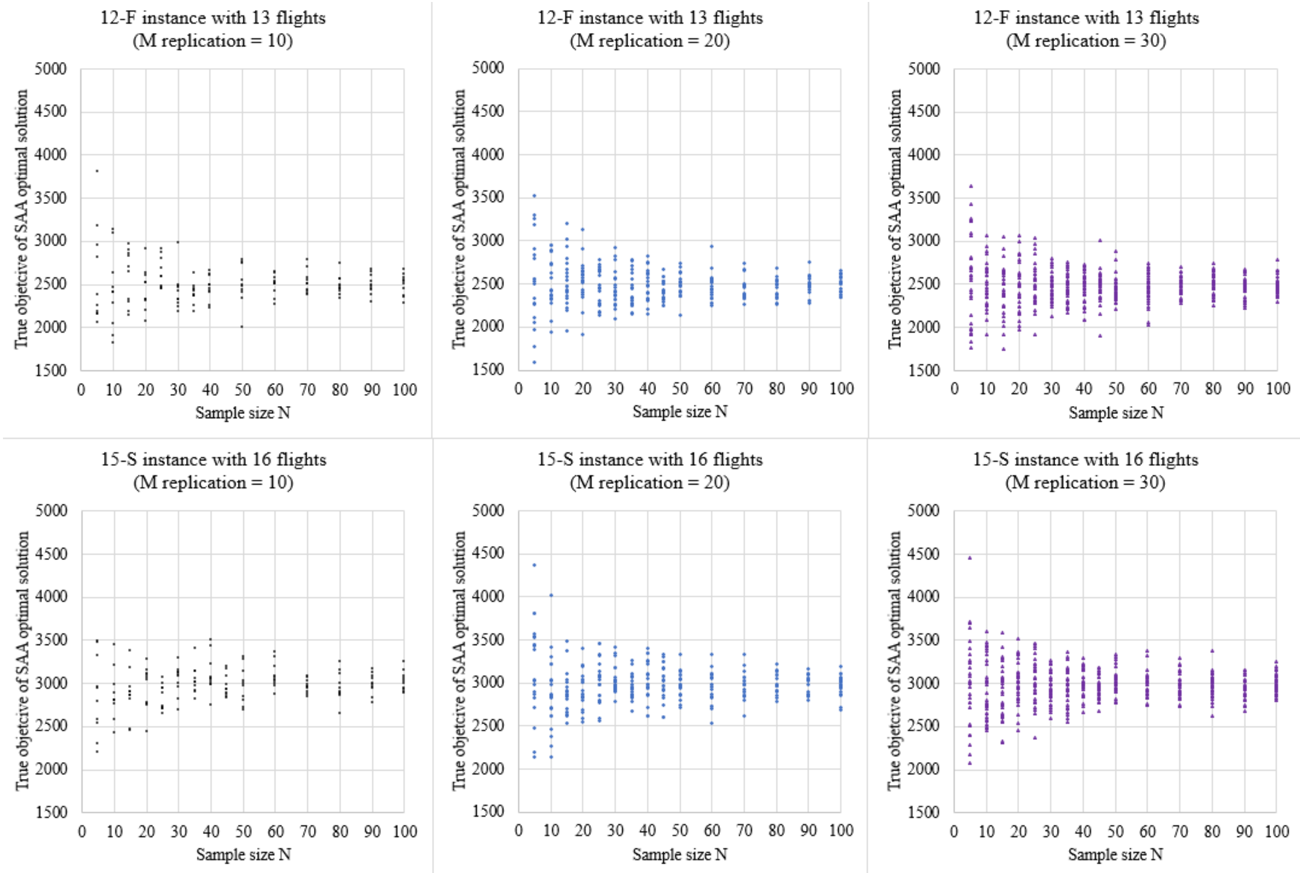

Fig. 16. Computational study on the effect of sample size N with replication M={10,20,30} using SAA

The computational study on the change of sample size N with M replication $M = \{10,20,30\}$ using SSA approach to solve 12-F and 15-S instances are presented in **Fig. 16**. The value v_N^m with sample size N are mapped and reveals that the degree of dispersion of the optimal value v_N^m tends to decrease when the sample size N is larger than 70 in the numerical study. **Fig. 17** presents the computational time with an increase of sample size N and replication M. The computational time of all the solutions for solving the instance 12-F is satisfied with the computational limit. The computational time is over 30 minutes for solving the instance 15-S with sample size $N = 100$ and replication $M = 30$, but replication $M = 20$ satisfied a computational requirement. The sample size $N = \{70,80,90,100\}$ and replication $M = \{10,20\}$ are the possible parameter settings for SAA according to the results of test instances.

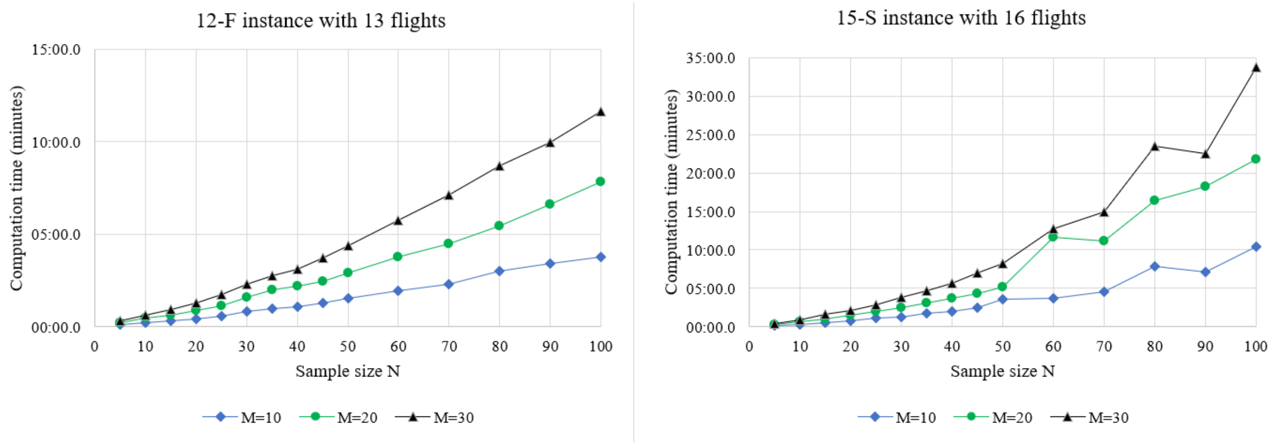

Fig. 17. Computation time on the effect of sample size N by M replication (M=10,20,30) using SAA

In **Table 4**, we solved the instances with $N' = 1500$ to obtain an estimated objective value and compare the estimated optimality gap θ. We observed that some of the estimated optimality gap with replication $M = 10$ for $N = \{70,80,90,100\}$ was over 2%. Therefore, we disregarded the consideration of choosing $M = 10$. The same issue could be found with replication $M = 20$ and sample size $N = \{70,80\}$. The performance of replication $M = 10$ and sample size $N = \{90,100\}$ for the setting of SAA algorithm is similar and the optimality gap is satisfied with less than or round 1%. Therefore, we concluded that the we adopted sample size $N = 90$ and replication $M = 20$ of the parameters setting of SAA algorithm for following the numerical analysis on real-world instances.

Table 4

Numerical results of the SAA method with $N' = 1500, M = \{10,20\}, N = \{70,80,90,100\}$

Instance 12-F		$M = 10$		$M = 20$	
Estimated objective value $G_{N'}(\overline{\varphi})$, where $N' = 1500$	N	Statistical lower bound $\overline{v}_N^M$	Estimated optimality gap θ	Statistical lower bound $\overline{v}_N^M$	Estimated optimality gap θ
2440.936	70	2526.32	3.38%	2493.135	2.09%
	80	2489.223	1.94%	2498.059	2.29%
	90	2500.36	2.38%	2443.874	0.12%
	100	2491.132	2.01%	2448.327	0.30%
Instance 15-S		$M = 10$		$M = 20$	
Estimated objective value $G_{N'}(\overline{\varphi})$, where $N' = 1500$	N	Statistical lower bound $\overline{v}_N^M$	Estimated optimality gap θ	Statistical lower bound $\overline{v}_N^M$	Estimated optimality gap θ
2944.584	70	2965.528	0.71%	2971.413	0.90%
	80	2964.226	0.66%	2996.366	1.73%
	90	2994.504	1.67%	2967.142	0.76%
	100	3027.35	2.73%	2974.894	1.02%

$\lambda = 0.5, \gamma = 3.0, \delta = 0$

5.3. Trade-off between efficiency loss and cruise speed acceleration/deceleration

The number of flights in the decision horizon ranges from 11 to 16 in the instances. According to the empirical distribution function of arrival lateness at entry waypoints in **Fig. 11**, the average lateness and average delay at entry waypoints are -

3.99 minutes and 13.98 minutes. In our numerical analysis, all instances achieved global optimum within computation time limit.

In the following analysis, we are interested in the effect of global optimum with different combination of efficiency loss γ and trade-off parameter λ. We fixed the additional buffer δ of longitudinal separation distance as zero. The set of efficiency loss is set to be $\gamma \in \{0.1, 0.12, 0.14, 0.16, 0.18, 0.20, 0.22, 0.24, 0.26, 0.28, 0.30\}$, while the set of trade-off parameter is denoted as $\lambda \in \{0.2, 0.4, 0.5, 0.6, 0.8\}$.

The results of average robustness cost, average delay cost and average penalty cost are shown in **Fig. 18Error! Reference source not found.**, **Fig. 19Error! Reference source not found.** and **Fig. 20Error! Reference source not found.**, respectively. In the computational analysis of SAA approach with 20th replications and 90 sample size in each replication, the efficiency loss $\gamma \in \{0.1, 0.12, 0.14\}$ yields infeasible solutions for all instances. Given a scenario with zero additional buffer on longitudinal separation distance $\delta = 0$ and the same λ value, the robustness cost, average delay cost and average penalty cost are almost unchanged with respect to the change of γ where $\gamma \in \{0.16, 0.18, 0.20, 0.22, 0.24, 0.26, 0.28, 0.30\}$. As expected, the change of efficiency loss γ only limits the feasible region and restrict the model with limited scratch of total delay cost and total penalty cost. In this regard, we can conclude that at least 14% runway efficiency from optimal value F^* is required to satisfy the impact of uncertain arrival time on entry waypoints.

The robustness cost is the convex combination of total delay cost and total penalty cost. In the objective function (43), $\lambda = 0.2$ implies that the total delay cost has a lower weighting, or vice versa. As shown in **Error! Reference source not found.**, **Error! Reference source not found.**, and **Error! Reference source not found.**, given the feasible solutions with the same γ, the average robustness cost, average delay cost and λ are positive correlated. One may notice that, in **Error! Reference source not found.**, the $\lambda = \{0.2, 0.4\}$ yielded a low value, while the average penalty cost for with the $\lambda = \{0.6, 0.8\}$ is slightly lower than the one with $\lambda = 0.5$. The penalty cost of cruise speed acceleration or deceleration is much more effective when solving the model with $\lambda = 0.5$. Given a higher value of λ, the results were not performed as expected. The total penalty cost may reach the capacity of longitudinal separation minima and it can only seize a portion of TMA capacity. Once it further seizes the TMA capacity, extra delay may induce to all subsequence's flights as "chain effect". In this regard, increase in landing time is much more effective.

In **Fig. 21**, **Fig. 22** and **Fig. 23**, we summarise the percentile (Q0: minimum, Q1: 25th quartile, Q2: 50th quartile, Q3: 75th quartile and Q4: maximum) of the robustness cost, delay cost and penalty cost with 20th replications and 90 sample size (1800 results in total). We fixed the parameters with $\lambda = 0.5, \gamma = 1$ and evaluate the solutions and their objective values with $\delta \in \{0, 1, 2, 3, 5, 10\}$ nautical miles. The longitudinal separation distance matrix, ranging from 3 to 7 nautical miles, is presented in (K. K. H. Ng, Lee, et al., 2020a) and is subject to the flight class of leading and following flights. All instances retrieved similar objective values with $\delta \in \{0, 1, 2, 3\}$ and we can expect that the solution with $\delta \in \{0, 1, 2, 3\}$ can increase the separation distance between flights and ensure a higher level of safety factor, meanwhile, the overall robustness cost would not change much. We may regard these solutions are robust and vulnerable to uncertain factors in TMA. For the solutions with $\delta \in \{5, 10\}$, the average robustness cost, delay cost and penalty cost may increase or decrease compared to the solutions with $\delta \in \{0, 1, 2, 3\}$. The results implied that a higher value of additional buffer may not increase or decrease the robustness cost, but subject to the scenarios, which depend on the TMA capacity, distance between flights and the traffic of each STAR.

5.4. Discussion

The proposed robust terminal traffic flow problem considering cruise speed adjustment and compensation of solution robustness and efficiency loss aims to improve vulnerability to air traffic disruption on arrival manager. ATC can firstly determine a robust arrival schedule in pre-tactical phase and then adjust the arrival schedule with respect to real-time variables from time to time. The near time decision in cruise speed adjustment can enjoy certain level of flexibility in the second-stage optimisation model. The lower and upper bounds of the cruise speed is formulated as a box interval and the decision makers can pre-adjust with respect to the dwell wind intensity and directions based on the historical meteorological data. Such adjustment will affect the value of the cruise speed limit and the levels of model flexibility.

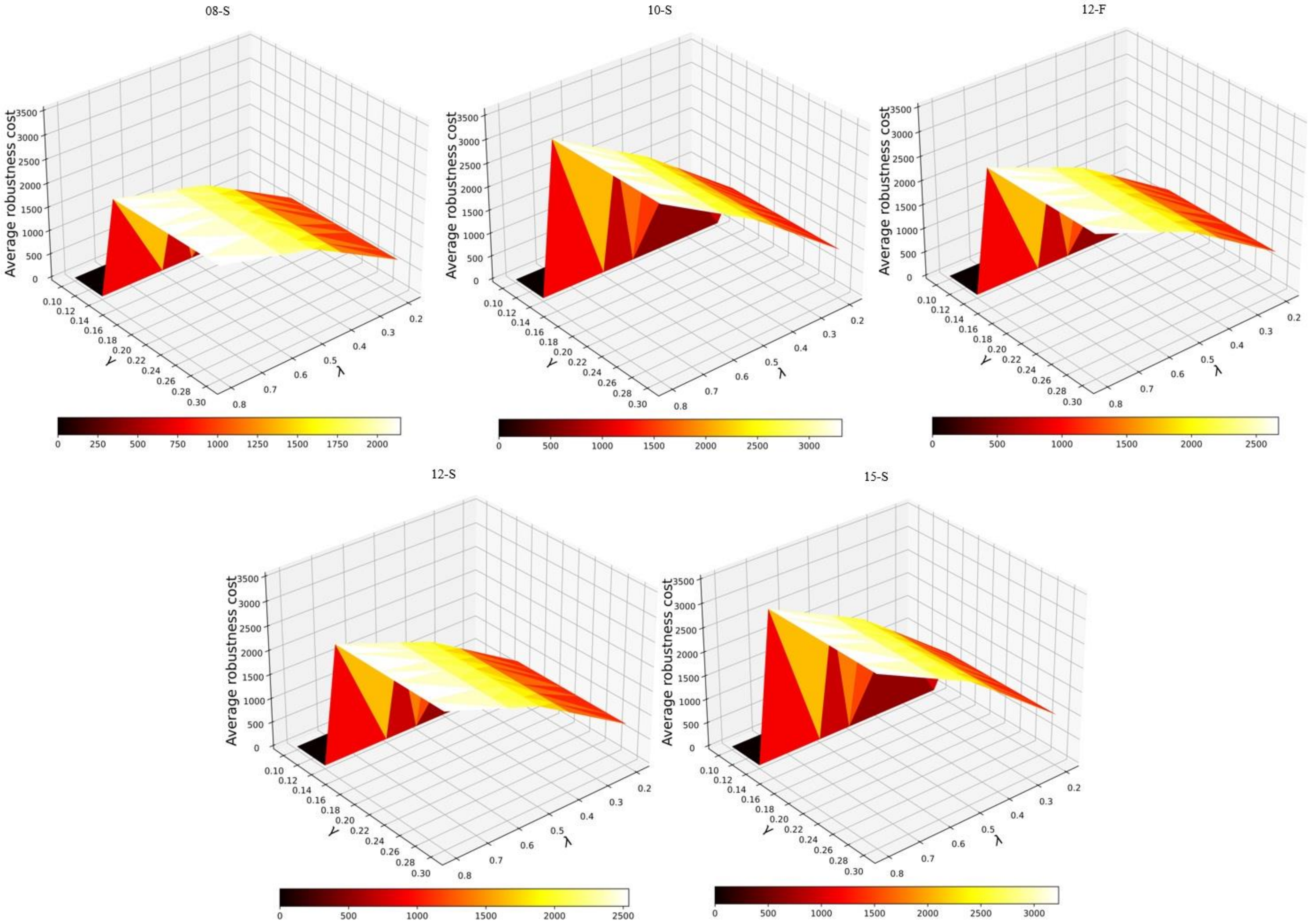

Fig. 18. Computational results of average robustness cost with the value changes of λ and γ and $\delta = 0$.

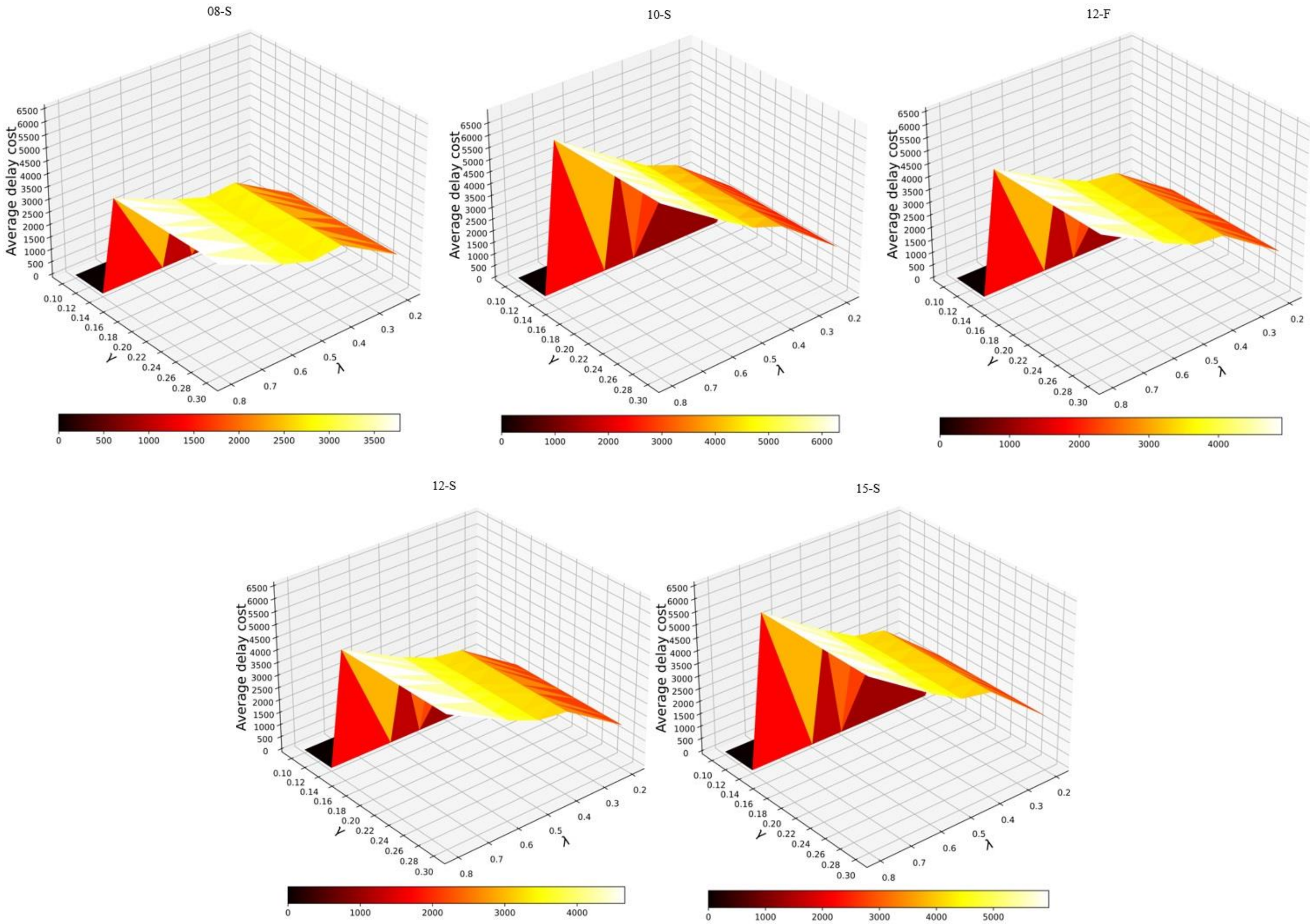

Fig. 19. Computational results of average delay cost with the value changes of λ and γ and $\delta = 0$.

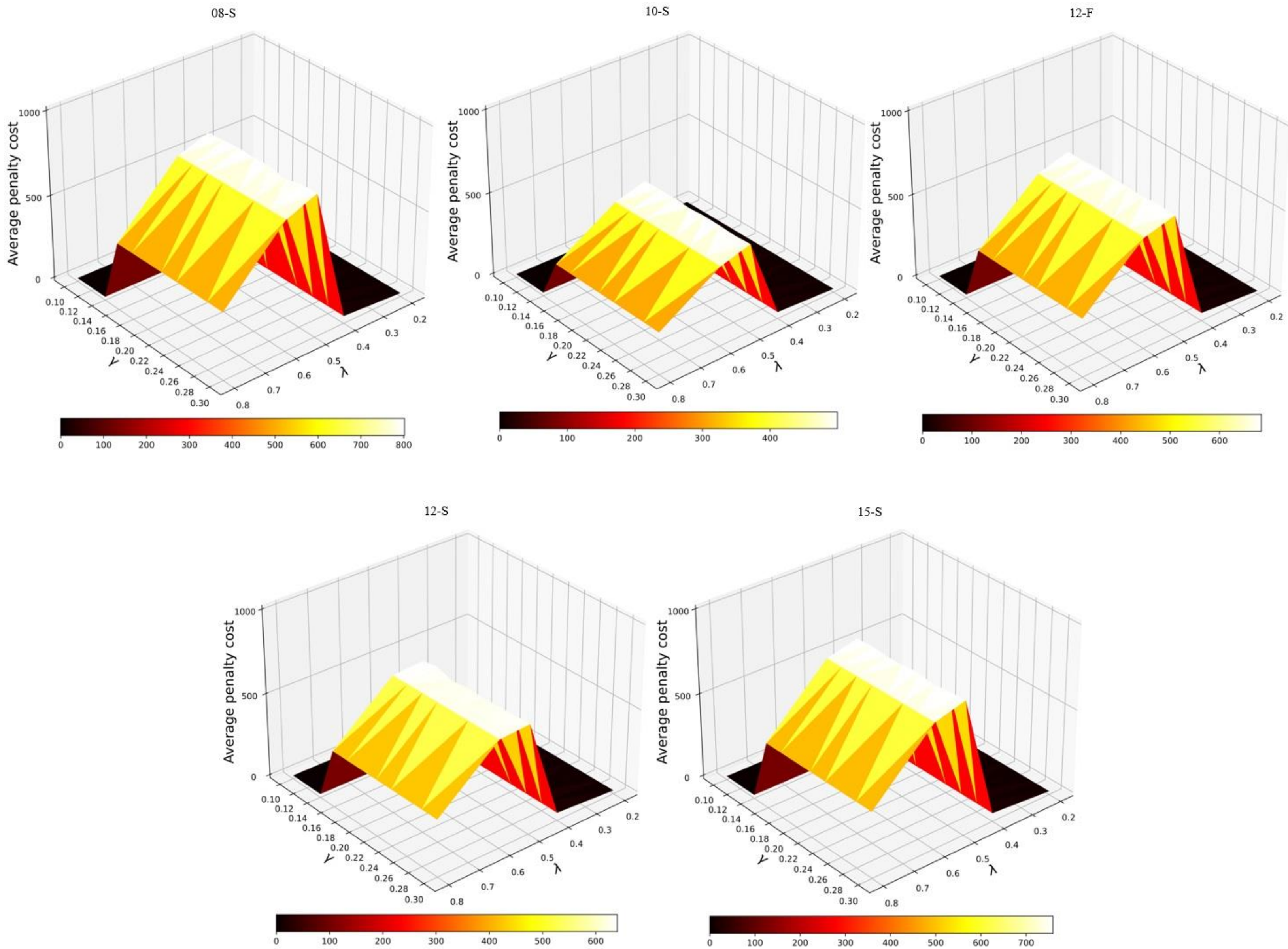

Fig. 20. Computational results of average penalty cost with the value changes of λ and γ and $\delta = 0$.

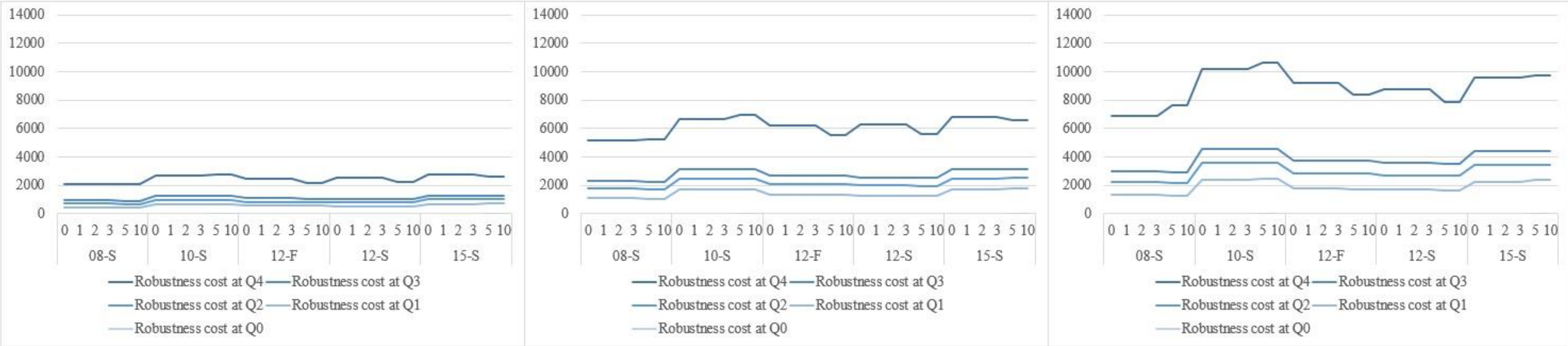

Fig. 21. Percentile of robustness cost with value changes of δ and $\lambda = 0.5, \gamma = 1$

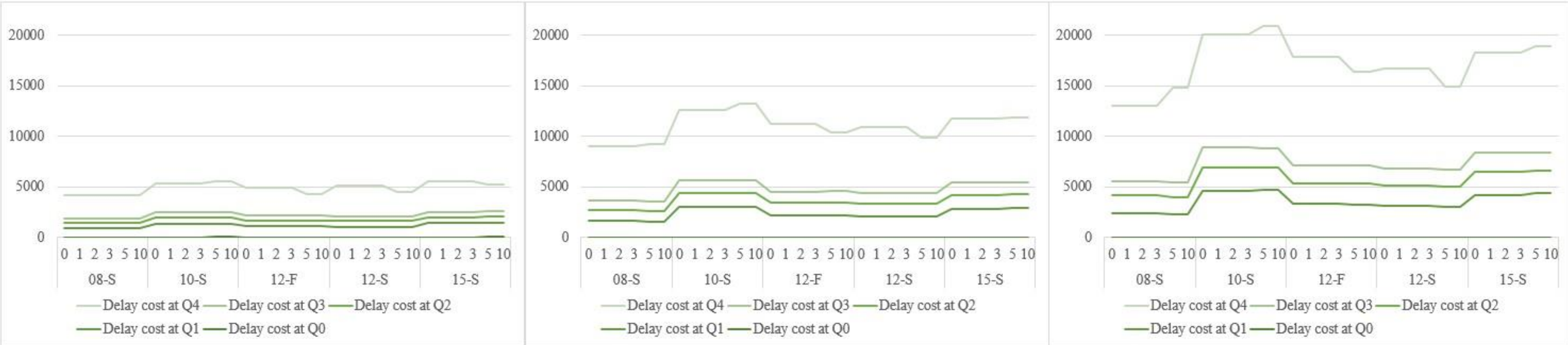

Fig. 22. Percentile of delay cost with value changes of δ and $\lambda = 0.5, \gamma = 1$

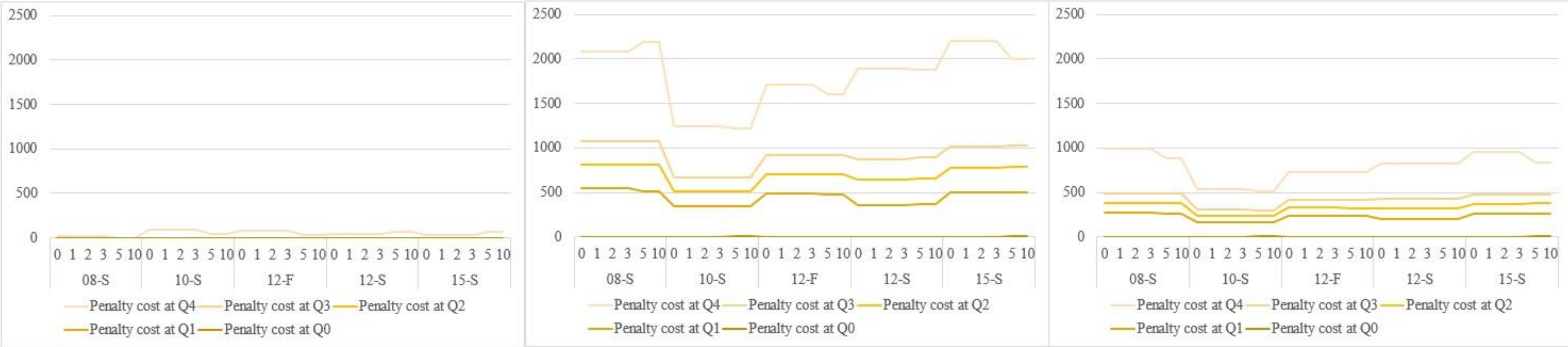

Fig. 23. Percentile of penalty cost with value changes of δ and $\lambda = 0.5, \gamma = 1$

6. Conclusion

This research illustrates a novel alternative path approach for the RSD-TTFP model with the consideration of cruise speed adjustment. The uncertainty of flight time addressed in this model presents the consequence of an approach route with unpleasant weather conditions and turbulence in a near TMA. The propagation of airside delay risks at the terminal area can be resolved by proper robust terminal traffic flow scheduling. With the introduction of uncertainty parameters in robust optimisation, the vulnerability to disruption could be further increased. Fault-driven re-scheduling efforts and aggregate delays can be alleviated and partially absorbed using the robust optimisation method in schedule design. Further, a better estimation of the impact and the consequence of uncertainty assists the ATCOs in developing a robust schedule with less effect on the change of predefined schedules and passenger unease if a precise decision with a risk-free approach is impossible to be adopted in actual operations.

To demonstrate the proposed method and validate the modelling in the numerical study, we adopted real-world data from the HKIA. The following conclusions regarding the results of the numerical experiments were arrived at.

- By introducing the uncertain arrival time at the entry waypoints for flights, the model identified that the primary delay at entry points led to an aggregated delay on the arrival time on runway. In our scenario analysis using SAA approach, the cruise speed adjustment reduced the total delay time on runway.
- The proposed solution procedure of robust schedule design for TTFP can include user-specific parameters and a decision-maker attitude while designing the solution. ATCOs can determine the additional buffer for longitudinal separation minima to increase the solution robustness and decide the trade-off between estimated average delay time and estimated penalty cost on cruise speed adjustment based on their preferences and anticipated traffic situation.
- In our numerical study, the efficiency loss from D-TTFP schedule was suggested to be 20% of the optimal value of the first-stage optimisation problem. The possible level of additional buffer of longitudinal separation requirement for medium-sized and large-sized instances can reach 10NM and 5NM, respectively. The trade-off parameter $\lambda = 0.6$ provided the best balance between average delay time and average penalty cost of cruise speed adjustment in our numerical experiments.

Several interesting research directions can be considered based on the work that has been done in this article. First, this research attempts to seize the resource utilisation in handling air traffic. We could also extend the consideration of other air routes and airport resources. With a proper evaluation of runway physical property, runways can be used in switch mode function. The runway configuration of a multi-runways system can adjust the current runway configuration between landing and take-off mode and match the arrival and departure demand. Second, in this research, we attempted to provide a method for achieving better solution robustness and operational efficiency based on minor perturbation of uncertain arrival time. One may also be interested in the resilience modelling in approaching decisions to handle major disruptions. Third, more advanced soft computing and optimisation methods, such as meta-heuristics, matheuristics and hyper-heuristics, can be considered for solving a complex model in a timely fashion. Fourth, the determination of empirical distribution function of arrival lateness at entry waypoints can be modelled as data-driven approach. The traffic demand correlation sensitive to time horizon and weather pattern can be further improved the prediction and applicability to actual scenarios. Meanwhile, the quality and quantity of historical traffic and weather data are highly associated with the prediction power of cost of robustness in TTFP. Forth, the flight descending approaches, e.g. continuous descent approach and optimised profile descent (OPD), can further improve the overall traffic volume as well as the fuel consumption. The integration of TTFP and flight trajectory profile is also an interesting research direction and benefit the ATC operations.

Appendix A. Computational results in details

Parameters		Average robustness cost					Average delay cost					Average penalty cost				
λ	γ	08-S	10-S	12-F	12-S	15-S	08-S	10-S	12-F	12-S	15-S	08-S	10-S	12-F	12-S	15-S
0.2	0.16	709.33	982.18	836.00	797.88	1003.06	1418.66	1964.28	1671.95	1595.71	2006.01	0.01	0.08	0.05	0.04	0.11
	0.18	709.35	982.17	836.00	797.89	1003.06	1418.69	1964.27	1671.96	1595.72	2006.00	0.01	0.08	0.05	0.05	0.12
	0.20	709.34	982.18	836.00	797.88	1003.08	1418.68	1964.28	1671.95	1595.72	2006.04	0.01	0.08	0.05	0.04	0.11
	0.22	709.34	982.18	836.01	797.88	1003.06	1418.67	1964.29	1671.97	1595.73	2006.00	0.01	0.08	0.05	0.03	0.11
	0.24	709.35	982.18	836.01	797.88	1003.07	1418.68	1964.26	1671.97	1595.73	2006.01	0.01	0.10	0.05	0.03	0.12
	0.26	709.33	982.18	836.00	797.88	1003.07	1418.66	1964.28	1671.96	1595.70	2006.02	0.01	0.08	0.05	0.06	0.11
	0.28	709.33	982.19	836.00	797.88	1003.07	1418.66	1964.28	1671.96	1595.70	2006.02	0.01	0.09	0.05	0.06	0.11
	0.30	709.35	982.18	836.00	797.88	1003.07	1418.68	1964.29	1671.96	1595.70	2006.02	0.01	0.08	0.05	0.06	0.12
0.4	0.16	1415.03	1960.32	1667.17	1591.04	2000.31	2806.11	3900.73	3306.59	3155.58	3970.11	23.94	19.92	27.75	26.50	30.50
	0.18	1415.00	1960.33	1667.17	1591.04	2000.30	2805.84	3900.66	3306.90	3155.40	3970.10	24.17	19.99	27.44	26.68	30.50
	0.20	1415.03	1960.34	1667.19	1591.03	2000.32	2805.98	3900.54	3306.76	3155.31	3970.05	24.08	20.13	27.62	26.74	30.58
	0.22	1415.02	1960.31	1667.16	1591.02	2000.29	2805.94	3900.71	3306.84	3155.22	3970.07	24.09	19.92	27.49	26.83	30.51
	0.24	1415.01	1960.34	1667.17	1591.01	2000.29	2805.81	3900.56	3306.76	3155.30	3970.53	24.20	20.13	27.58	26.73	30.05
	0.26	1415.02	1960.34	1667.18	1591.02	2000.28	2806.00	3900.74	3306.83	3155.40	3970.48	24.03	19.94	27.52	26.64	30.08
	0.28	1415.01	1960.32	1667.17	1591.03	2000.29	2805.92	3900.64	3306.79	3155.20	3970.20	24.10	20.00	27.55	26.87	30.38
	0.30	1415.01	1960.33	1667.18	1591.02	2000.30	2805.72	3900.53	3306.85	3155.35	3970.24	24.29	20.13	27.51	26.68	30.35
0.5	0.16	1762.80	2445.29	2076.71	1982.16	2492.22	2709.75	4375.24	3449.99	3324.56	4211.64	815.85	515.33	703.43	639.77	772.80
	0.18	1762.79	2445.29	2076.69	1982.19	2492.23	2702.06	4371.87	3451.50	3308.55	4204.96	823.51	518.70	701.88	655.84	779.51
	0.20	1762.80	2445.34	2076.68	1982.16	2492.23	2696.03	4371.90	3444.63	3341.30	4215.39	829.58	518.78	708.74	623.02	769.06
	0.22	1762.81	2445.29	2076.70	1982.17	2492.22	2702.63	4378.87	3451.58	3328.82	4213.06	822.98	511.71	701.82	635.52	771.38
	0.24	1762.82	2445.32	2076.70	1982.16	2492.25	2696.33	4372.83	3454.07	3334.21	4204.27	829.31	517.81	699.33	630.10	780.23
	0.26	1762.82	2445.31	2076.70	1982.16	2492.23	2722.83	4374.61	3459.15	3329.71	4222.93	802.82	516.01	694.25	634.61	761.53
	0.28	1762.80	2445.28	2076.68	1982.15	2492.23	2698.12	4380.65	3450.30	3327.69	4209.68	827.49	509.90	703.05	636.61	774.79
	0.30	1762.83	2445.31	2076.70	1982.15	2492.25	2700.56	4375.74	3460.29	3326.29	4207.82	825.09	514.88	693.12	638.01	776.69
0.6	0.16	1928.01	2819.89	2332.35	2223.43	2810.63	3104.31	5179.02	4022.72	3821.36	4894.72	751.71	460.76	641.97	625.50	726.54
	0.18	1928.02	2819.88	2332.33	2223.44	2810.61	3104.23	5179.02	4022.79	3820.97	4894.51	751.80	460.74	641.87	625.92	726.71
	0.20	1927.99	2819.87	2332.31	2223.44	2810.64	3104.26	5178.84	4022.58	3821.18	4894.83	751.73	460.90	642.05	625.69	726.45
	0.22	1928.00	2819.88	2332.31	2223.44	2810.63	3104.36	5178.80	4022.46	3821.33	4894.79	751.64	460.96	642.15	625.55	726.46
	0.24	1928.00	2819.86	2332.34	2223.40	2810.63	3104.24	5178.90	4022.69	3821.09	4894.84	751.76	460.82	642.00	625.71	726.42
	0.26	1928.00	2819.85	2332.35	2223.43	2810.62	3104.29	5178.85	4022.73	3821.27	4894.70	751.70	460.85	641.97	625.59	726.53
	0.28	1927.98	2819.88	2332.33	2223.43	2810.60	3104.06	5179.08	4022.72	3821.48	4894.68	751.90	460.67	641.94	625.37	726.52
	0.30	1927.99	2819.86	2332.30	2223.41	2810.61	3104.29	5178.75	4022.61	3821.26	4894.62	751.68	460.96	641.98	625.55	726.61
0.8	0.16	2254.56	3565.65	2838.96	2699.36	3440.17	4127.60	6896.83	5350.01	5077.25	6507.85	381.51	234.46	327.91	321.47	372.49
	0.18	2254.57	3565.68	2838.98	2699.39	3440.18	4127.60	6896.88	5349.97	5077.25	6507.73	381.54	234.49	327.99	321.53	372.64
	0.20	2254.56	3565.67	2838.96	2699.37	3440.16	4127.58	6896.88	5350.02	5077.29	6507.75	381.54	234.46	327.90	321.45	372.57
	0.22	2254.55	3565.63	2838.96	2699.34	3440.17	4127.60	6896.76	5349.96	5077.26	6507.84	381.49	234.50	327.95	321.42	372.49
	0.24	2254.52	3565.69	2838.94	2699.37	3440.16	4127.60	6896.84	5349.96	5077.26	6507.80	381.44	234.54	327.93	321.49	372.53
	0.26	2254.55	3565.65	2841.68	2699.36	3440.16	4127.60	6896.81	5354.94	5077.26	6507.78	381.49	234.49	328.43	321.47	372.55
	0.28	2254.55	3565.66	2841.68	2699.37	3440.14	4127.60	6896.89	5354.94	5077.26	6507.70	381.50	234.43	328.43	321.49	372.58
	0.30	2254.55	3565.66	2841.69	2699.39	3440.13	4127.61	6896.82	5354.93	5077.26	6507.74	381.49	234.50	328.46	321.52	372.53

References

Aissi, H., Bazgan, C., & Vanderpooten, D. (2009). Min–max and min–max regret versions of combinatorial optimization problems: A survey. *European Journal of Operational Research, 197*(2), 427-438. doi:https://doi.org/10.1016/j.ejor.2008.09.012

Artiouchine, K., Baptiste, P., & Dürr, C. (2008). Runway sequencing with holding patterns. *European Journal of Operational Research, 189*(3), 1254-1266. doi:https://doi.org/10.1016/j.ejor.2006.06.076

Balakrishnan, H., & Chandran, B. G. (2010). Algorithms for Scheduling Runway Operations Under Constrained Position Shifting. *Operations Research, 58*(6), 1650-1665. doi:10.1287/opre.1100.0869

Ball, M., Barnhart, C., Dresner, M., Hansen, M., Neels, K., Odoni, A., . . . Zou, B. (2010). *Total delay impact study.* Paper presented at the NEXTOR Research Symposium, Washington DC.

Ball, M. O., Hansen, M., Swaroop, P., & Zou, B. (2013). Design and Justification for Market-Based Approaches to Airport Congestion Management. In *Modelling and Managing Airport Performance* (pp. 259-277): John Wiley & Sons.

Basso, L. J. (2008). Airport deregulation: Effects on pricing and capacity. *International Journal of Industrial Organization, 26*(4), 1015-1031. doi:http://dx.doi.org/10.1016/j.ijindorg.2007.09.002

Ben-Tal, A., Bertsimas, D., & Brown, D. B. (2010). A soft robust model for optimization under ambiguity. *Operations research, 58*(4-part-2), 1220-1234.

Bertsimas, D., Lulli, G., & Odoni, A. (2011). An integer optimization approach to large-scale air traffic flow management. *Operations research, 59*(1), 211-227.

Bertsimas, D., Nohadani, O., & Teo, K. M. (2010). Robust optimization for unconstrained simulation-based problems. *Operations research, 58*(1), 161-178.

Bianco, L., Dell'Olmo, P., & Giordani, S. (1997). Scheduling Models and Algorithms for TMA Traffic Management. In L. Bianco, P. Dell'Olmo, & A. R. Odoni (Eds.), *Modelling and Simulation in Air Traffic Management* (pp. 139-167). Berlin, Heidelberg: Springer Berlin Heidelberg.

Cacchiani, V., & Toth, P. (2012). Nominal and robust train timetabling problems. *European Journal of Operational Research, 219*(3), 727-737. doi:https://doi.org/10.1016/j.ejor.2011.11.003

Campanelli, B., Fleurquin, P., Arranz, A., Etxebarria, I., Ciruelos, C., Eguíluz, V. M., & Ramasco, J. J. (2016). Comparing the modeling of delay propagation in the US and European air traffic networks. *Journal of Air Transport Management, 56*, 12-18. doi:http://dx.doi.org/10.1016/j.jairtraman.2016.03.017

Chen, X., Shapiro, A., & Sun, H. (2019). Convergence analysis of sample average approximation of two-stage stochastic generalized equations. *SIAM Journal on Optimization, 29*(1), 135-161.

Chen, X., Yu, H., Cao, K., Zhou, J., Wei, T., & Hu, S. (2020). Uncertainty-Aware Flight Scheduling for Airport Throughput and Flight Delay Optimization. *IEEE Transactions on Aerospace and Electronic Systems, 56*(2), 853-862. doi:10.1109/TAES.2019.2921193

Churchill, A., Lovell, D., & Ball, M. (2010). Flight Delay Propagation Impact on Strategic Air Traffic Flow Management. *Transportation Research Record: Journal of the Transportation Research Board, 2177*, 105-113. doi:10.3141/2177-13

De La Vega, J., Munari, P., & Morabito, R. (2020). Exact approaches to the robust vehicle routing problem with time windows and multiple deliverymen. *Computers & Operations Research, 124*, 105062. doi:https://doi.org/10.1016/j.cor.2020.105062

Delavernhe, F., Lersteau, C., Rossi, A., & Sevaux, M. (2020). Robust scheduling for target tracking using wireless sensor networks. *Computers & Operations Research, 116*, 104873. doi:https://doi.org/10.1016/j.cor.2019.104873

Deng, W., Zhao, H., Yang, X., Li, D., Li, Y., & Liu, J. (2018). Research on a robust multi-objective optimization model of gate assignment for hub airport. *Transportation Letters, 10*(4), 229-241. doi:10.1080/19427867.2016.1252876

Epstein, L. G. (1999). A Definition of Uncertainty Aversion. *The Review of Economic Studies, 66*(3), 579-608. Retrieved from http://www.jstor.org/stable/2567015

Eun, Y., Hwang, I., & Bang, H. (2010). Optimal arrival flight sequencing and scheduling using discrete airborne delays. *IEEE Transactions on Intelligent Transportation Systems, 11*(2), 359-373.

Farhadi, F., Ghoniem, A., & Al-Salem, M. (2014). Runway capacity management–an empirical study with application to Doha International Airport. *Transportation Research Part E: Logistics and Transportation Review, 68*, 53-63.

Fischetti, M., Salvagnin, D., & Zanette, A. (2009). Fast approaches to improve the robustness of a railway timetable. *Transportation Science, 43*(3), 321-335.

García-Heredia, D., Alonso-Ayuso, A., & Molina, E. (2019). A Combinatorial model to optimize air traffic flow management problems. *Computers & Operations Research, 112*, 104768. doi:https://doi.org/10.1016/j.cor.2019.104768

Gehlot, H., Honnappa, H., & Ukkusuri, S. V. (2020). An optimal control approach to day-to-day congestion pricing for stochastic transportation networks. *Computers & Operations Research, 119*, 104929. doi:https://doi.org/10.1016/j.cor.2020.104929

Gelhausen, M. C., Berster, P., & Wilken, D. (2013). Do airport capacity constraints have a serious impact on the future development of air traffic? *Journal of Air Transport Management, 28*, 3-13. doi:http://dx.doi.org/10.1016/j.jairtraman.2012.12.004

Gilboa, I., & Schmeidler, D. (1989). Maxmin expected utility with non-unique prior. *Journal of Mathematical Economics, 18*(2), 141-153. doi:https://doi.org/10.1016/0304-4068(89)90018-9

Gillen, D., Jacquillat, A., & Odoni, A. R. (2016). Airport demand management: The operations research and economics perspectives and potential synergies. *Transportation Research Part A: Policy and Practice, 94*, 495-513. doi:https://doi.org/10.1016/j.tra.2016.10.011

Givoni, M., & Chen, X. (2017). Airline and railway disintegration in China: the case of Shanghai Hongqiao Integrated Transport Hub. *Transportation Letters, 9*(4), 202-214. doi:10.1080/19427867.2016.1252877

Habibi, M. K. K., Battaïa, O., Cung, V.-D., Dolgui, A., & Tiwari, M. K. (2019). Sample average approximation for multi-vehicle collection–disassembly problem under uncertainty. *International Journal of Production Research, 57*(8), 2409-2428. doi:10.1080/00207543.2018.1519262

Hansen, M., & Zou, B. (2013). Airport Operational Performance and Its Impact on Airline Cost. In *Modelling and Managing Airport Performance* (pp. 119-143): John Wiley & Sons.

He, C., Guan, Z., Xu, G., Yue, L., & Ullah, S. (2020). Scenario-based robust dominance criteria for multi-objective automated flexible transfer line balancing problem under uncertainty. *International Journal of Production Research, 58*(2), 467-486. doi:10.1080/00207543.2019.1593549

Heidt, A., Helmke, H., Kapolke, M., Liers, F., & Martin, A. (2016). Robust runway scheduling under uncertain conditions. *Journal of Air Transport Management, 56*, 28-37. doi:https://doi.org/10.1016/j.jairtraman.2016.02.009

Högdahl, J., Bohlin, M., & Fröidh, O. (2019). A combined simulation-optimization approach for minimizing travel time and delays in railway timetables. *Transportation Research Part B: Methodological, 126*, 192-212. doi:https://doi.org/10.1016/j.trb.2019.04.003

Hong, Y., Choi, B., & Kim, Y. (2018). Two-Stage Stochastic Programming Based on Particle Swarm Optimization for Aircraft Sequencing and Scheduling. *IEEE Transactions on Intelligent Transportation Systems, 20*(4), 1365-1377.

Hong, Y., Choi, B., Lee, K., & Kim, Y. (2018). Dynamic Robust Sequencing and Scheduling Under Uncertainty for the Point Merge System in Terminal Airspace. *IEEE Transactions on Intelligent Transportation Systems, 19*(9), 2933-2943. doi:10.1109/TITS.2017.2766683

Hu, H., Ng, K. K. H., & Qin, Y. (2016). Robust Parallel Machine Scheduling Problem with Uncertainties and Sequence-Dependent Setup Time. *Scientific Programming, 2016*, 13. doi:10.1155/2016/5127253

Jacquillat, A., & Odoni, A. R. (2015a). Endogenous control of service rates in stochastic and dynamic queuing models of airport congestion. *Transportation Research Part E: Logistics and Transportation Review, 73*, 133-151. doi:http://dx.doi.org/10.1016/j.tre.2014.10.014

Jacquillat, A., & Odoni, A. R. (2015b). An Integrated Scheduling and Operations Approach to Airport Congestion Mitigation. *Operations Research, 63*(6), 1390-1410. doi:https://doi.org/10.1287/opre.2015.1428

Jacquillat, A., & Odoni, A. R. (2018). A roadmap toward airport demand and capacity management. *Transportation Research Part A: Policy and Practice, 114*, 168-185. doi:https://doi.org/10.1016/j.tra.2017.09.027

Jacquillat, A., Odoni, A. R., & Webster, M. D. (2016). Dynamic control of runway configurations and of arrival and departure service rates at JFK airport under stochastic queue conditions. *Transportation Science, 51*(1), 155-176.

Jacquillat, A., Odoni, A. R., & Webster, M. D. (2017). Dynamic Control of Runway Configurations and of Arrival and Departure Service Rates at JFK Airport Under Stochastic Queue Conditions. *Transportation Science, 51*(1), 155-176. doi:https://doi.org/10.1287/trsc.2015.0644

Kafle, N., & Zou, B. (2016). Modeling flight delay propagation: A new analytical-econometric approach. *Transportation Research Part B: Methodological, 93*, 520-542. doi:http://dx.doi.org/10.1016/j.trb.2016.08.012

Khan, W. A., Chung, S.-H., Ma, H.-L., Liu, S. Q., & Chan, C. Y. (2019). A novel self-organizing constructive neural network for estimating aircraft trip fuel consumption. *Transportation Research Part E: Logistics and Transportation Review, 132*, 72-96. doi:https://doi.org/10.1016/j.tre.2019.10.005

Kleywegt, A. J., Shapiro, A., & Homem-de-Mello, T. (2002). The sample average approximation method for stochastic discrete optimization. *SIAM Journal on Optimization, 12*(2), 479-502.

Lee, C. K., Zhang, S., & Ng, K. K. (2019). Design of An Integration Model for Air Cargo Transportation Network Design and Flight Route Selection. *Sustainability, 11*(19), 5197.

Lee, C. K. M., Ng, K. K. H., Chan, H. K., Choy, K. L., Tai, W. C., & Choi, L. S. (2018). A multi-group analysis of social media engagement and loyalty constructs between full-service and low-cost carriers in Hong Kong. *Journal of Air Transport Management, 73*, 46-57. doi:https://doi.org/10.1016/j.jairtraman.2018.08.009

Li, X., & Zhang, K. (2018). A sample average approximation approach for supply chain network design with facility disruptions. *Computers & Industrial Engineering, 126*, 243-251. doi:https://doi.org/10.1016/j.cie.2018.09.039

Liang, M., Delahaye, D., & Marechal, P. (2018). Conflict-free arrival and departure trajectory planning for parallel runway with advanced point-merge system. *Transportation Research Part C: Emerging Technologies, 95*, 207-227. doi:https://doi.org/10.1016/j.trc.2018.07.006

Liang, Z., Xiao, F., Qian, X., Zhou, L., Jin, X., Lu, X., & Karichery, S. (2018). A column generation-based heuristic for aircraft recovery problem with airport capacity constraints and maintenance flexibility. *Transportation Research Part B: Methodological, 113*, 70-90. doi:https://doi.org/10.1016/j.trb.2018.05.007

Lieder, A., Briskorn, D., & Stolletz, R. (2015). A dynamic programming approach for the aircraft landing problem with

aircraft classes. *European Journal of Operational Research, 243*(1), 61-69. doi:https://doi.org/10.1016/j.ejor.2014.11.027
Lieder, A., & Stolletz, R. (2016). Scheduling aircraft take-offs and landings on interdependent and heterogeneous runways. *Transportation Research Part E: Logistics and Transportation Review, 88*, 167-188. doi:http://dx.doi.org/10.1016/j.tre.2016.01.015
Long, Y., Lee, L. H., & Chew, E. P. (2012). The sample average approximation method for empty container repositioning with uncertainties. *European Journal of Operational Research, 222*(1), 65-75. doi:https://doi.org/10.1016/j.ejor.2012.04.018
Lu, Z., Zhu, H., Han, X., & Hu, X. (2019). Integrated modelling and algorithm of material delivery and line-side storage for aircraft moving assembly lines. *International Journal of Production Research, 57*(18), 5842-5856. doi:10.1080/00207543.2018.1554917
Lusby, R. M., Larsen, J., & Bull, S. (2018). A survey on robustness in railway planning. *European Journal of Operational Research, 266*(1), 1-15. doi:https://doi.org/10.1016/j.ejor.2017.07.044
Maiyar, L. M., & Thakkar, J. J. (2019). Robust optimisation of sustainable food grain transportation with uncertain supply and intentional disruptions. *International Journal of Production Research*, 1-25. doi:10.1080/00207543.2019.1656836
Marla, L., Vaze, V., & Barnhart, C. (2018). Robust optimization: Lessons learned from aircraft routing. *Computers & Operations Research, 98*, 165-184. doi:https://doi.org/10.1016/j.cor.2018.04.011
Murça, M. C. R., Hansman, R. J., Li, L., & Ren, P. (2018). Flight trajectory data analytics for characterization of air traffic flows: A comparative analysis of terminal area operations between New York, Hong Kong and Sao Paulo. *Transportation Research Part C: Emerging Technologies, 97*, 324-347. doi:https://doi.org/10.1016/j.trc.2018.10.021
Ng, K. K. H., Chen, C.-H., & Lee, C. K. M. (2020). Mathematical programming formulations for robust airside terminal traffic flow optimisation problem. *Computers & Industrial Engineering*.
Ng, K. K. H., Chen, C.-H., & Lee, C. K. M. (2021). Mathematical programming formulations for robust airside terminal traffic flow optimisation problem. *Computers & Industrial Engineering, 154*, 107119. doi:https://doi.org/10.1016/j.cie.2021.107119
Ng, K. K. H., Lee, C. K., Chan, F. T., Chen, C.-H., & Qin, Y. (2020a). A two-stage robust optimisation for terminal traffic flow problem. *Applied Soft Computing, 89*, 106048.
Ng, K. K. H., Lee, C. K. M., Chan, F. T. S., Chen, C.-H., & Qin, Y. (2020b). A two-stage robust optimisation for terminal traffic flow problem. *Applied Soft Computing, 89*, 106048. doi:https://doi.org/10.1016/j.asoc.2019.106048
Ng, K. K. H., Lee, C. K. M., Chan, F. T. S., & Lv, Y. (2018). Review on meta-heuristics approaches for airside operation research. *Applied Soft Computing, 66*, 104-133. doi:https://doi.org/10.1016/j.asoc.2018.02.013
Ng, K. K. H., Lee, C. K. M., Chan, F. T. S., & Qin, Y. (2017). Robust aircraft sequencing and scheduling problem with arrival/departure delay using the min-max regret approach. *Transportation Research Part E: Logistics and Transportation Review, 106*, 115-136. doi:https://doi.org/10.1016/j.tre.2017.08.006
Nikoleris, T., & Hansen, M. (2012). Queueing models for trajectory-based aircraft operations. *Transportation Science, 46*(4), 501-511.
Peterson, E. B., Neels, K., Barczi, N., & Graham, T. (2013). The economic cost of airline flight delay. *Journal of Transport Economics and Policy (JTEP), 47*(1), 107-121.
Pohl, M., Kolisch, R., & Schiffer, M. (2020). Runway scheduling during winter operations. *Omega*, 102325. doi:https://doi.org/10.1016/j.omega.2020.102325
Pour, A. G., Naji-Azimi, Z., & Salari, M. (2017). Sample average approximation method for a new stochastic personnel assignment problem. *Computers & Industrial Engineering, 113*, 135-143. doi:https://doi.org/10.1016/j.cie.2017.09.006
Prakash, R., Piplani, R., & Desai, J. (2018). An optimal data-splitting algorithm for aircraft scheduling on a single runway to maximize throughput. *Transportation Research Part C: Emerging Technologies, 95*, 570-581. doi:https://doi.org/10.1016/j.trc.2018.07.031
Pyrgiotis, N., Malone, K. M., & Odoni, A. (2013). Modelling delay propagation within an airport network. *Transportation Research Part C: Emerging Technologies, 27*, 60-75. doi:http://dx.doi.org/10.1016/j.trc.2011.05.017
Qian, X., Mao, J., Chen, C.-H., Chen, S., & Yang, C. (2017). Coordinated multi-aircraft 4D trajectories planning considering buffer safety distance and fuel consumption optimization via pure-strategy game. *Transportation Research Part C: Emerging Technologies, 81*, 18-35. doi:https://doi.org/10.1016/j.trc.2017.05.008
Qin, Y., Chan, F. T. S., Chung, S. H., Qu, T., & Niu, B. (2018). Aircraft parking stand allocation problem with safety consideration for independent hangar maintenance service providers. *Computers & Operations Research, 91*, 225-236. doi:https://doi.org/10.1016/j.cor.2017.10.001
Qin, Y., Wang, Z. X., Chan, F. T. S., Chung, S. H., & Qu, T. (2018). A Family of Heuristic-Based Inequalities for Maximizing Overall Safety Margins in Aircraft Parking Stands Arrangement Problems. *Mathematical Problems in Engineering, 2018*, 16. doi:10.1155/2018/3525384
Qin, Y., Wang, Z. X., Chan, F. T. S., Chung, S. H., & Qu, T. (2019). A mathematical model and algorithms for the aircraft

hangar maintenance scheduling problem. *Applied Mathematical Modelling, 67*, 491-509. doi:https://doi.org/10.1016/j.apm.2018.11.008

Qiu, R., Sun, Y., & Sun, M. (2020). A Distributionally Robust Optimization Approach for Multi-Product Inventory Decisions with Budget Constraint and Demand and Yield Uncertainties. *Computers & Operations Research*, 105081. doi:https://doi.org/10.1016/j.cor.2020.105081

Sáez, R., Polishchuk, T., Schmidt, C., Hardell, H., Smetanová, L., Polishchuk, V., & Prats, X. (2021). Automated sequencing and merging with dynamic aircraft arrival routes and speed management for continuous descent operations. *Transportation Research Part C: Emerging Technologies, 132*, 103402. doi:https://doi.org/10.1016/j.trc.2021.103402

Sáez, R., Prats, X., Polishchuk, T., & Polishchuk, V. (2020). Traffic synchronization in terminal airspace to enable continuous descent operations in trombone sequencing and merging procedures: An implementation study for Frankfurt airport. *Transportation Research Part C: Emerging Technologies, 121*, 102875. doi:https://doi.org/10.1016/j.trc.2020.102875

Samà, M., D'Ariano, A., Corman, F., & Pacciarelli, D. (2018). Coordination of scheduling decisions in the management of airport airspace and taxiway operations. *Transportation Research Part A: Policy and Practice, 114*, 398-411. doi:https://doi.org/10.1016/j.tra.2018.01.028

Samà, M., D'Ariano, A., Corman, F., & Pacciarelli, D. (2017). Metaheuristics for efficient aircraft scheduling and re-routing at busy terminal control areas. *Transportation Research Part C: Emerging Technologies, 80*, 485-511. doi:https://doi.org/10.1016/j.trc.2016.08.012

Samà, M., D'Ariano, A., D'Ariano, P., & Pacciarelli, D. (2014). Optimal aircraft scheduling and routing at a terminal control area during disturbances. *Transportation Research Part C: Emerging Technologies, 47*, 61-85. doi:http://dx.doi.org/10.1016/j.trc.2014.08.005

Samà, M., D'Ariano, A., D'Ariano, P., & Pacciarelli, D. (2017). Scheduling models for optimal aircraft traffic control at busy airports: Tardiness, priorities, equity and violations considerations. *Omega, 67*, 81-98. doi:https://doi.org/10.1016/j.omega.2016.04.003

Samà, M., D'Ariano, A., & Pacciarelli, D. (2013a). Rolling Horizon Approach for Aircraft Scheduling in the Terminal Control Area of Busy Airports. *Procedia - Social and Behavioral Sciences, 80*, 531-552. doi:http://dx.doi.org/10.1016/j.sbspro.2013.05.029

Samà, M., D'Ariano, A., & Pacciarelli, D. (2013b). Rolling horizon approach for aircraft scheduling in the terminal control area of busy airports. *Transportation Research Part E: Logistics and Transportation Review, 60*, 140-155. doi:https://doi.org/10.1016/j.tre.2013.05.006

Schmeidler, D. (1989). Subjective Probability and Expected Utility without Additivity. *Econometrica, 57*(3), 571-587. doi:10.2307/1911053

Sinclair, K., Cordeau, J.-F., & Laporte, G. (2014). Improvements to a large neighborhood search heuristic for an integrated aircraft and passenger recovery problem. *European Journal of Operational Research, 233*(1), 234-245. doi:http://dx.doi.org/10.1016/j.ejor.2013.08.034

Singham, D. I. (2019). Sample average approximation for the continuous type principal-agent problem. *European Journal of Operational Research, 275*(3), 1050-1057. doi:https://doi.org/10.1016/j.ejor.2018.12.032

Tang, C.-H., & Wang, Y.-W. (2020). Transportation outsourcing problems considering feasible probabilities under stochastic demands. *Computers & Operations Research*, 105109. doi:https://doi.org/10.1016/j.cor.2020.105109

Toratani, D. (2019). Application of merging optimization to an arrival manager algorithm considering trajectory-based operations. *Transportation Research Part C: Emerging Technologies, 109*, 40-59. doi:https://doi.org/10.1016/j.trc.2019.09.015

Vink, J., Santos, B. F., Verhagen, W. J. C., Medeiros, I., & Filho, R. (2020). Dynamic aircraft recovery problem - An operational decision support framework. *Computers & Operations Research, 117*, 104892. doi:https://doi.org/10.1016/j.cor.2020.104892

Wang, S., & Meng, Q. (2012). Robust schedule design for liner shipping services. *Transportation Research Part E: Logistics and Transportation Review, 48*(6), 1093-1106. doi:https://doi.org/10.1016/j.tre.2012.04.007

Wee, H. J., Lye, S. W., & Pinheiro, J.-P. (2018). A Spatial, Temporal Complexity Metric for Tactical Air Traffic Control. *The Journal of Navigation*, 1-15.

Xu, L., Zhang, C., Xiao, F., & Wang, F. (2017). A robust approach to airport gate assignment with a solution-dependent uncertainty budget. *Transportation Research Part B: Methodological, 105*, 458-478. doi:https://doi.org/10.1016/j.trb.2017.09.013

Xu, X., Cui, W., Lin, J., & Qian, Y. (2013). Robust makespan minimisation in identical parallel machine scheduling problem with interval data. *International Journal of Production Research, 51*(12), 3532-3548. doi:10.1080/00207543.2012.751510

Yan, S., & Chen, Y.-C. (2021). Flight rescheduling, fleet rerouting and passenger reassignment for typhoon disruption events. *Transportation Letters*, 1-20. doi:10.1080/19427867.2021.1950266

Yang, Y., Gao, Z., & He, C. (2020). Stochastic terminal flight arrival and departure scheduling problem under performance-based navigation environment. *Transportation Research Part C: Emerging Technologies, 119*, 102735.

doi:https://doi.org/10.1016/j.trc.2020.102735
Zheng, S., Yang, Z., He, Z., Wang, N., Chu, C., & Yu, H. (2019). Hybrid simulated annealing and reduced variable neighbourhood search for an aircraft scheduling and parking problem. *International Journal of Production Research*, 1-21. doi:10.1080/00207543.2019.1629663
Zou, B., & Hansen, M. (2012). Impact of operational performance on air carrier cost structure: Evidence from US airlines. *Transportation Research Part E: Logistics and Transportation Review, 48*(5), 1032-1048. doi:http://dx.doi.org/10.1016/j.tre.2012.03.006